Universidade de Aveiro Departamento de Química
2014

CATARINA MAIA SECO SEIÇA NEVES

TRATAMENTO DE EFLUENTES AQUOSOS CONTAMINADOS COM LÍQUIDOS IÓNICOS

TREATMENT OF AQUEOUS EFFLUENTS CONTAMINATED WITH IONIC LIQUIDS

APPENDIX

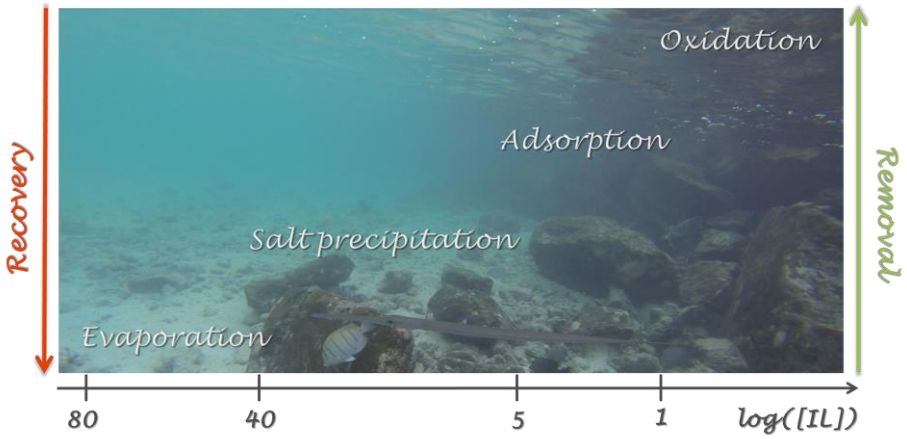

Universidade de Aveiro Departamento de Química
2014

CATARINA MAIA SECO SEIÇA NEVES

TRATAMENTO DE EFLUENTES AQUOSOS CONTAMINADOS COM LÍQUIDOS IÓNICOS

TREATMENT OF AQUEOUS EFFLUENTS CONTAMINATED WITH IONIC LIQUIDS

Tese apresentada à Universidade de Aveiro para cumprimento dos requisitos necessários à obtenção do grau de Doutor em Química, realizada sob a orientação científica do Professor Doutor. João Manuel da Costa e Araújo Pereira Coutinho, Professor Catedrático do Departamento de Química da Universidade de Aveiro, e coorientação da Doutora Mara Guadalupe Freire Martins, Investigadora Coordenadora no Departamento de Química, CICECO, da Universidade de Aveiro

Apoio financeiro do POCTI no âmbito do III Quadro Comunitário de Apoio. Cofinanciamento do POPH/FSE.

O doutorando agradece o apoio financeiro da FCT no âmbito do III Quadro Comunitário de Apoio (SFRH / BD / 70641 / 2010).

Contents

List of Figures

List of Tables

Appendix Chapter 2 – Ionic-Liquid-based Processes

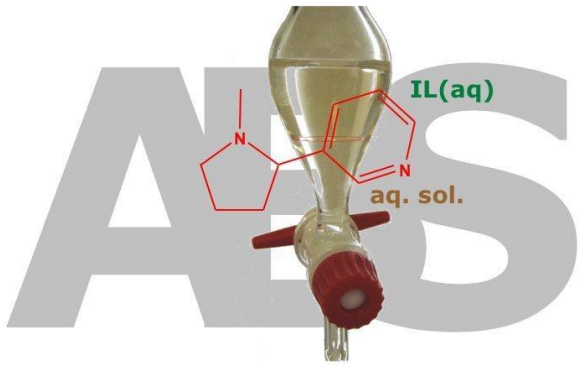

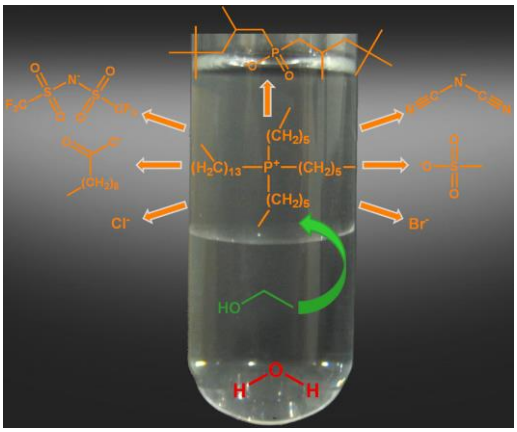

2.1. High-performance extraction of alkaloids using aqueous two-phase systems with ionic liquids

Mara G. Freire, Catarina M. S. S. Neves, Isabel M. Marrucho, José N. Canongia Lopes, Luís Paulo N. Rebelo and João A. P. Coutinho, Green Chemistry 12 (2010) 1715-1718, DOI: 10.1039/c0gc00179a

EXPERIMENTAL PROCEDURE

Nicotine, > 99 wt% pure, was purchased from Sigma-Aldrich while caffeine, > 98.5 wt% pure, was acquired at Marsing & Co. Ltd. A/S. All ionic liquids (ILs) were commercially acquired at Iolitec, with the exception of $[C_4C_1im][CF_3CO_2]$ that was purchased from Solchemar. Ionic liquids individual samples were dried under constant conditions at moderate vacuum and temperature, for a minimum of 48 h, before use. The purity of each ionic liquid was further checked by ^{1}H, ^{13}C, and ^{19}F NMR spectra and found to be superior to 99 wt% for all samples. Urea, 99 wt% pure, was supplied by Panreac and used without further purification. K_3PO_4, 98 wt% pure, and NaCl, 99.9 % wt% pure, were from Sigma and Normapur, respectively. In order to remove water, the inorganic salts were dried under vacuum for a minimum of 12 h before use. Water used was ultrapure water, double distilled, passed by a reverse osmosis system and finally treated with a Milli-Q plus 185 water purification equipment.

Synthetic human urine aqueous phases were prepared by dissolution of urea and NaCl, in pure water, at the concentrations of 1.2 $g \cdot dm^{-3}$ and 4.0 $g \cdot dm^{-3}$, respectively. The alkaloids quantification, in both phases, was carried out by UV spectroscopy using a SHIMADZU UV-1700, Pharma-Spec spectrometer, at a wavelength of 274 nm or 261 nm for caffeine and nicotine, respectively, and using calibration curves previously established. Initial concentrations of caffeine and nicotine for phase distribution at the water ternary composition were, respectively, 2.6×10^{-2} $mol \cdot dm^{-3}$ and 2.5×10^{-2} $mol \cdot dm^{-3}$. Possible interferences of both the inorganic salt and the ionic liquid with the analytical method were taken into account and blank controls were employed whenever necessary. The partition coefficients of caffeine (K_{caf}) or nicotine (K_{nic}) are defined as the ratio between

the concentration of the alkaloids in the IL- and K_3PO_4-rich phases.Partition Coefficients and Extraction Efficiencies

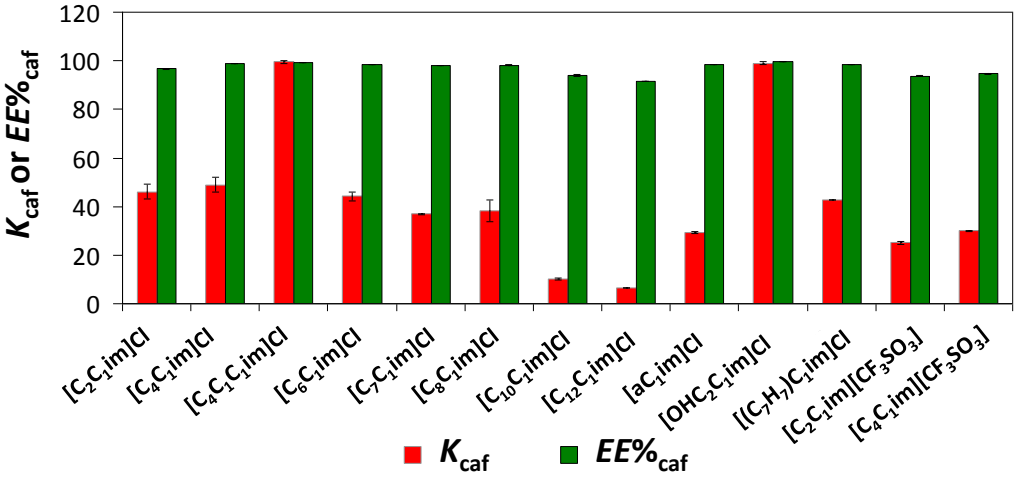

Figure S 2.1. Partition coefficients (K_{caf}) and extraction efficiencies percentages ($EE\%_{caf}$) of caffeine in chloride-based ILs/K_3PO_4 ABS at 298 K (IL at 25 wt% and K_3PO_4 at 15 wt%, except for $[(C_7H_7)C_1im]Cl$ at 40 wt% and K_3PO_4 at 15 wt%).

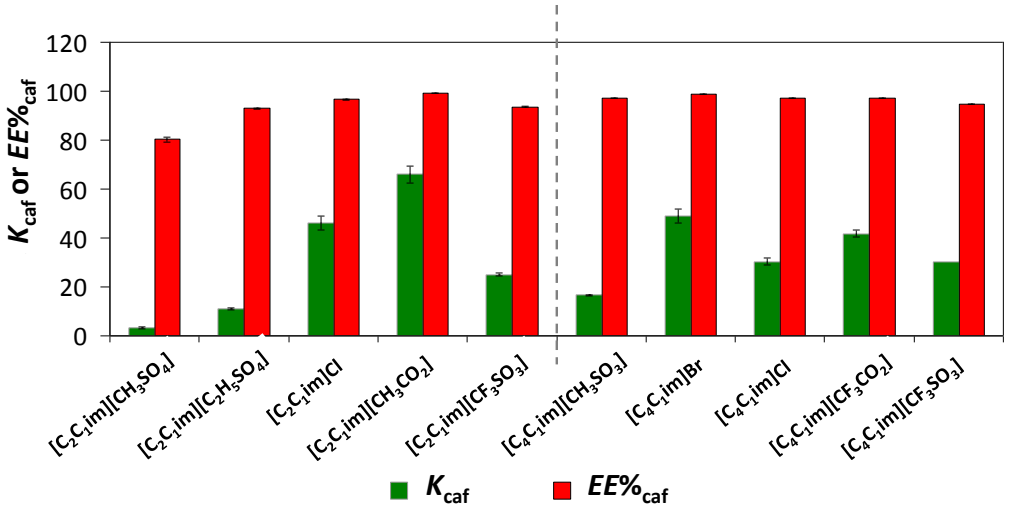

Figure S 2.2. Partition coefficients (K_{caf}) and extraction efficiencies percentages ($EE\%_{caf}$) of caffeine in $[C_2C_1im]$- and $[C_4C_1im]$-based ILs/K_3PO_4 ABS at 298 K (IL at 25 wt% and K_3PO_4).

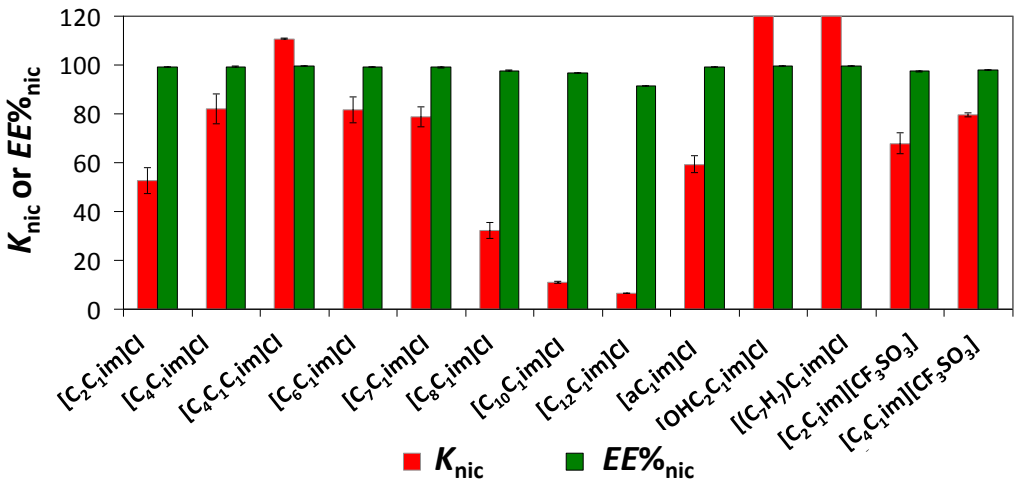

Figure S 2.3. Partition coefficients (K_{nic}) and extraction efficiencies percentages ($EE\%_{nic}$) of nicotine in chloride-based ILs/K_3PO_4 ABS at 298 K (IL at 25 wt% and K_3PO_4 at 15 wt%, except for [(C_7H_7)C_1im]Cl at 40 wt% and K_3PO_4 at 15 wt%).

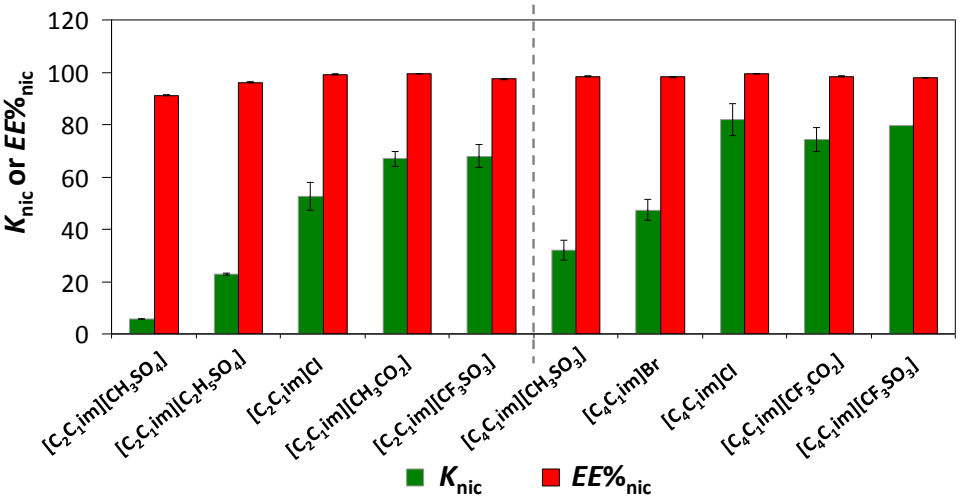

Figure S 2.4. Partition coefficients (K_{nic}) and extraction efficiencies percentages ($EE\%_{nic}$) of nicotine in [C_2C_1im]- and [C_4C_1im]-based ILs/K_3PO_4 ABS at 298 K (IL at 25 wt% and K_3PO_4).

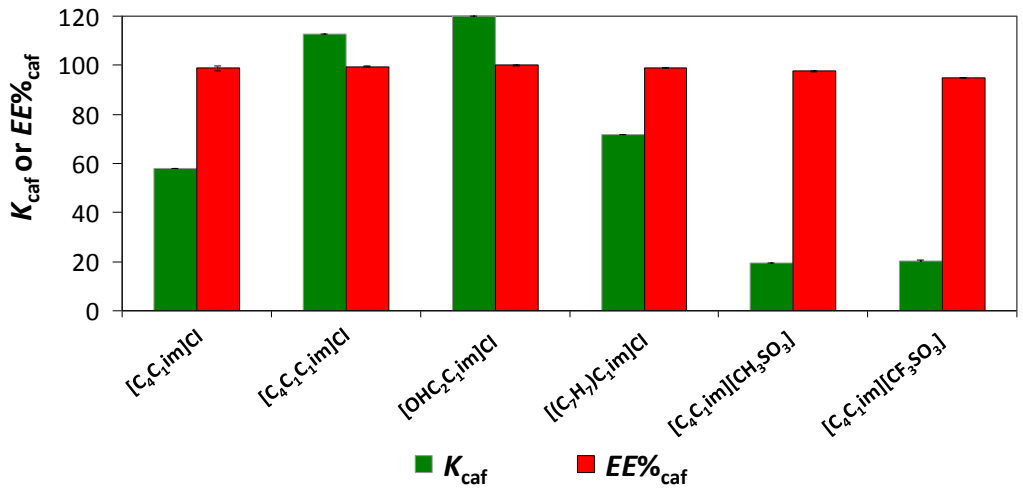

Figure S 2.5. Partition coefficients (K_{caf}) and extraction efficiencies percentages ($EE\%_{caf}$) of caffeine in human urine-based ILs/K_3PO_4 ABS at 298 K (IL at 25 wt% and K_3PO_4 at 15 wt%, except for $[(C_7H_7)C_1im]Cl$ at 40 wt% and K_3PO_4 at 15 wt%).

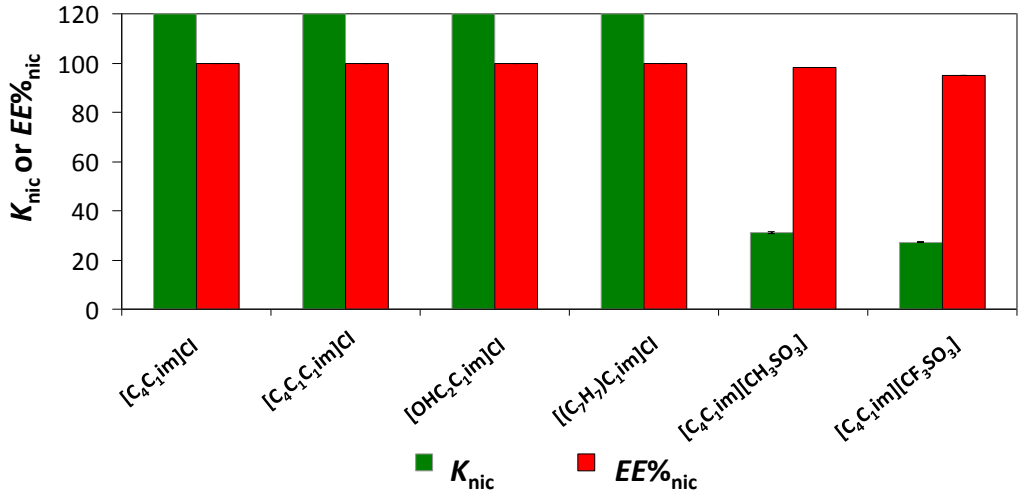

Figure S 2.6. Partition coefficients (K_{nic}) and extraction efficiencies percentages ($EE\%_{nic}$) of nicotine in human urine-based ILs/K_3PO_4 ABS at 298 K (IL at 25 wt% and K_3PO_4 at 15 wt%, except for $[(C_7H_7)C_1im]Cl$ at 40 wt% and K_3PO_4 at 15 wt%).

Table S 2.1. Weight fraction composition, partition coefficients and extraction efficiencies of caffeine in IL-based ABS and respective tie-lines (TLs) and tie-line lengths (TLLs).

IL	wt%		TL equation IL (wt%) = $a + b \cdot K_3PO_4$ (wt%)		TLL	$K_{caf} \pm \sigma^a$	$EE\%_{caf} \pm \sigma^a$
	IL	K_3PO_4	a	b			
$[C_2C_1im]Cl$	25.185	14.962	42.205	-1.138	43.386	46.1 ± 2.9	96.70 ± 0.20
	40.093	15.129	58.722	-1.231	73.811	120	100
$[C_4C_1im]Cl$	24.361	14.923	42.269	-1.200	44.493	49.0 ± 2.9	98.89 ± 0.07
	30.320	14.760	49.407	-1.293	57.788	120	100

	34.989	15.479	55.708	-1.339	67.523	120	100
	39.855	15.004	59.968	-1.341	73.856	120	100
	44.853	15.040	66.399	-1.433	80.650	120	100
$[C_4C_1C_1im]Cl$	25.127	15.080	44.154	-1.262	47.966	99.6 ± 0.6	99.41 ± 0.03
$[C_6C_1im]Cl$	24.921	14.856	46.455	-1.450	45.907	44.1 ± 1.8	98.53 ± 0.06
$[C_7C_1im]Cl$	25.066	15.166	49.496	-1.611	44.417	37.0 ± 0.2	97.96 ± 0.01
$[C_8C_1im]Cl$	25.068	15.073	50.675	-1.699	36.784	38.2 ± 4.6	98.16 ± 0.22
$[C_{10}C_1im]Cl$	25.046	15.207	53.181	-1.850	24.853	10.1 ± 0.5	94.01 ± 0.26
$[C_{12}C_1im]Cl$	25.038	15.014	51.344	-1.752	27.518	6.65 ± 0.01	91.61 ± 0.01
	24.262	15.293	42.449	-1.189	42.842	29.4 ± 0.3	98.32 ± 0.02
	30.023	14.813	47.901	-1.207	56.670	120	100
$[aC_1im]Cl$	35.148	14.956	54.115	-1.268	66.449	120	100
	40.132	14.871	60.586	-1.375	73.839	120	100
	44.817	15.193	64.543	-1.298	81.148	32.3 ± 0.3	98.47 ± 0.04
$[OHC_2C_1im]Cl$	39.963	15.049	85.826	-3.048	63.673	98.9 ± 0.6	99.69 ± 0.02
	25.123	14.925	50.512	-1.701	43.036	42.62 ± 0.06	98.26 ± 0.02
	30.105	14.962	55.816	-1.718	56.054	120	100
	34.893	15.001	60.784	-1.726	65.219	120	100
	40.057	14.930	66.055	-1.741	73.246	120	100
$[(C_7H_7)C_1im]Cl$	44.996	14.930	69.071	-1.613	79.476	120	100
	49.962	14.883	75.540	-1.719	86.458	90.0 ± 5.7	99.51 ± 0.04
	25.152	19.997	59.596	-1.723	63.229	120	100
	25.053	25.067	66.647	-1.659	75.361	120	100
	25.130	29.832	71.663	-1.560	83.829	120	100
$[C_2C_1im][CF_3SO_3]$	24.996	14.891	69.540	-2.991	61.973	25.1 ± 0.8	93.59 ± 0.18
$[C_4C_1im][CF_3SO_3]$	24.996	15.352	70.967	-2.995	70.428	30.0 ± 0.2	94.70 ± 0.04
$[C_2C_1im][CH_3SO_4]$	25.007	15.178	51.644	-1.755	31.551	3.3 ± 0.5	80.27 ± 1.05
$[C_2C_1im][C_2H_5SO_4]$	24.853	15.648	54.162	-1.873	44.687	11.1 ± 0.3	92.86 ± 0.18
$[C_2C_1im][CH_3CO_2]$	25.172	14.931	39.995	-0.993	48.132	66.0 ± 3.6	99.34 ± 0.04
$[C_4C_1im]Br$	24.822	15.085	50.345	-1.692	45.396	30.4 ± 1.3	97.18 ± 0.11
$[C_4C_1im][CH_3SO_3]$	24.917	15.090	44.622	-1.306	38.919	16.6 ± 0.2	96.98 ± 0.04
$[C_4C_1im][CF_3CO_2]$	24.785	15.475	58.626	-2.187	56.984	41.8 ± 1.6	97.09 ± 0.14

[a]associated standard deviation

Table S 2.2. Weight fraction composition, partition coefficients and extraction efficiencies of nicotine in IL-based ABS and respective tie-lines (TLs) and tie-line lengths (TLLs).

IL	wt%		TL equation IL (wt%) = $a + b \cdot K_3PO_4$ (wt%)		TLL	$K_{nic} \pm \sigma^a$	$EE\%_{nic} \pm \sigma^a$
	IL	K_3PO_4	*a*	*b*			
$[C_2C_1im]Cl$	25.292	14.778	41.527	-1.099	43.583	52.7 ± 5.3	99.18 ± 0.08
	40.093	15.129	51.916	-1.237	73.950	58.7 ± 2.7	99.31 ± 0.03
$[C_4C_1im]Cl$	25.569	14.882	43.662	-1.216	47.673	82.1 ± 6.1	99.34 ± 0.05
	29.990	16.281	51.758	-1.337	60.914	120	100
	35.005	15.271	56.611	-1.415	67.114	120	100
	39.832	14.876	60.539	-1.392	73.521	120	100
	45.014	15.279	66.739	-1.422	81.312	120	100
	49.957	15.159	71.248	-1.405	87.410	95.5 ± 1.3	99.51 ± 0.03
$[C_4C_1C_1im]Cl$	25.007	15.170	44.057	-1.256	47.953	110.7 ± 0.2	99.47 ± 0.01
$[C_6C_1im]Cl$	25.125	14.891	47.112	-1.477	46.634	81.7 ± 5.4	99.17 ± 0.05
$[C_7C_1im]Cl$	25.014	15.263	49.737	-1.620	44.798	78.8 ± 4.0	99.01 ± 0.05
$[C_8C_1im]Cl$	25.010	15.079	50.901	-1.717	36.597	32.1 ± 3.3	97.71 ± 0.23
$[C_{10}C_1im]Cl$	24.992	15.146	53.162	-1.860	23.302	11.0 ± 0.3	96.72 ± 0.09
$[C_{12}C_1im]Cl$	25.000	15.010	51.576	-1.771	27.095	6.5 ± 0.1	91.49 ± 0.10
$[aC_1im]Cl$	24.945	15.198	43.838	-1.773	44.833	59.3 ± 3.6	99.17 ± 0.05
	29.895	14.931	47.853	-1.203	56.717	120	100
	34.916	15.013	53.812	-1.259	66.201	120	100
	39.761	15.222	53.383	-1.223	74.348	120	100
	45.146	15.093	63.720	-1.231	81.772	120	100
$[OHC_2C_1im]Cl$	40.072	14.915	86.128	-3.088	63.369	120	100
$[(C_7H_7)C_1im]Cl$	25.081	14.807	50.444	-1.691	43.240	120	100
	30.100	15.043	47.689	-1.169	54.397	120	100
	35.183	15.013	60.969	-1.718	65.685	120	100
	40.873	15.017	65.921	-1.668	74.182	120	100
	45.070	14.987	69.977	-1.662	79.952	120	100
	49.923	15.001	73.733	-1.554	86.007	120	100
	25.081	14.807	50.444	-1.691	43.241	120	100
	24.991	20.053	59.757	-1.734	63.292	120	100
	25.047	25.021	66.908	-1.673	75.522	120	100
	25.222	30.159	74.701	-1.641	86.515	120	100
$[C_2C_1im][CF_3SO_3]$	24.983	15.124	70.755	-3.027	63.646	67.9 ± 4.4	97.46 ± 0.16
$[C_4C_1im][CF_3SO_3]$	25.080	14.957	67.901	-2.863	65.409	79.6 ± 0.9	97.89 ± 0.02
$[C_2C_1im][CH_3SO_4]$	24.846	14.670	49.547	-1.684	24.412	5.7 ± 0.2	91.17 ± 0.22
$[C_2C_1im][C_2H_5SO_4]$	24.185	16.381	52.733	-1.743	45.780	22.8 ± 0.5	96.12 ± 0.08

$[C_2C_1im][CH_3CO_2]$	24.933	15.571	39.046	-0.936	48.787	66.9 ± 2.9	99.28 ± 0.03
$[C_4C_1im]Br$	25.046	14.937	50.237	-1.686	45.300	47.3 ± 4.0	98.24 ± 0.15
$[C_4C_1im][CH_3SO_3]$	24.998	14.979	44.769	-1.320	38.511	32.1 ± 3.8	98.38 ± 0.19
$[C_4C_1im][CF_3CO_2]$	24.933	14.779	56.326	-2.124	53.478	74.2 ± 4.7	98.47 ± 0.10

[a]associated standard deviation

Table S 2.3. Weight fraction composition, partition coefficients and extraction efficiencies, of caffeine and nicotine, in human urine-based ILs/K3PO4 ABS at 298 K.

IL	wt%		$K_{caf} \pm \sigma^a$	$EE\%_{caf} \pm \sigma^a$	wt%		$K_{nic} \pm \sigma^a$	$EE\%_{nic} \pm \sigma^a$
	IL	K_3PO_4			IL	K_3PO_4		
$[C_4C_1im]Cl$	25.117	14.997	57.8 ± 0.1	98.80 ± 0.01	24.844	14.937	120	100
$[C_4C_1C_1im]Cl$	24.896	15.119	112.7 ± 0.5	99.45 ± 0.07	24.889	15.275	120	100
$[OHC_2C_1im]Cl$	40.224	14.891	120	100	40.235	15.046	120	100
$[(C_7H_7)C_1im]Cl$	24.952	15.096	71.8 ± 0.2	98.88 ± 0.01	24.891	15.057	120	100
$[C_4C_1im][CH_3SO_3]$	25.050	14.982	19.3 ± 0.5	97.51 ± 0.07	24.837	15.513	31.1 ± 0.3	98.27 ± 0.02
$[C_4C_1im][CF_3SO_3]$	24.959	15.078	20.2 ± 1.7	94.97 ± 0.41	24.902	15.281	27.2 ± 0.2	94.95 ± 0.03

[a]associated standard deviation

2.2. Separation of ethanol-water mixtures by liquid-liquid extraction using phosphonium-based ionic liquids

Catarina M.S.S. Neves, José F.O. Granjo, Mara G. Freire, Al Robertson, Nuno M. C. Oliveira and João A. P. Coutinho, Green Chemistry 13 (2011) 1517-1526, DOI: 10.1039/C1GC15079K

EXPERIMENTAL DATA OF THE TERNARY SYSTEMS IL + WATER + ETOH

Table S 2.4. Experimental data and critical point calculated by the Sherwood method[1] for the ternary systems composed of IL + H_2O + EtOH.

IL	Phase	Mass Fraction			Selectivity (*S*)
		w_{IL}	w_{EtOH}	w_{H2O}	
$[P_{66614}][Phosph]$		0.840	0.000	0.160	
	Top	0.356	0.449	0.195	1.74
	Bottom	0.053	0.539	0.408	
	Top	0.524	0.335	0.141	3.13
	Bottom	0.001	0.432	0.567	
	Top	0.620	0.255	0.125	4.39
	Bottom	0.001	0.317	0.682	

	Top	0.718	0.161	0.121	5.68
	Bottom	0.000	0.190	0.810	
	Critical Point	0.18	0.54	0.28	
$[P_{66614}][Deca]$		0.851	0.000	0.149	
	Top	0.392	0.419	0.189	2.00
	Bottom	0.032	0.509	0.459	
	Top	0.513	0.341	0.146	3.09
	Bottom	0.003	0.429	0.568	
	Top	0.615	0.256	0.129	4.34
	Bottom	0.000	0.315	0.685	
	Top	0.716	0.162	0.122	5.31
	Bottom	0.000	0.201	0.799	
	Critical Point	0.21	0.55	0.24	
$[P_{66614}]Cl$		0.866	0.000	0.134	
	Top	0.438	0.395	0.167	2.24
	Bottom	0.079	0.472	0.449	
	Top	0.620	0.271	0.109	5.28
	Bottom	0.000	0.319	0.681	
	Top	0.807	0.082	0.111	6.61
	Bottom	0.000	0.100	0.900	
	Top	0.723	0.175	0.102	6.97
	Bottom	0.000	0.198	0.802	
	Critical Point	0.25	0.49	0.26	
$[P_{66614}][CH_3SO_3]$		0.872	0.000	0.128	
	Top	0.590	0.257	0.153	2.29
	Bottom	0.031	0.306	0.663	
	Top	0.703	0.176	0.121	3.64
	Bottom	0.006	0.218	0.776	
	Top	0.510	0.305	0.185	5.18
	Bottom	0.088	0.381	0.531	
	Top	0.795	0.085	0.120	6.67
	Bottom	0.004	0.096	0.900	
	Critical Point	0.40	0.37	0.23	
$[P_{66614}]Br$		0.932	0.000	0.068	
	Top	0.128	0.572	0.300	0.566
	Bottom	0.448	0.426	0.126	

	Top	0.054	0.555	0.391	2.74
	Bottom	0.562	0.348	0.090	
	Top	0.645	0.280	0.075	4.73
	Bottom	0.010	0.436	0.554	
	Top	0.718	0.223	0.059	7.76
	Bottom	0.001	0.326	0.673	
	Critical Point	0.28	0.53	0.19	
$[P_{66614}][N(CN)_2]$		0.967	0.000	0.033	
	Top	0.434	0.458	0.108	1.69
	Bottom	0.114	0.634	0.252	
	Top	0.622	0.313	0.065	3.41
	Bottom	0.020	0.574	0.406	
	Top	0.712	0.238	0.050	5.48
	Bottom	0.009	0.463	0.528	
	Top	0.787	0.169	0.044	7.76
	Bottom	0.008	0.330	0.662	
	Critical Point	0.28	0.16	0.56	
$[P_{66614}][NTf_2]$		0.998	0.000	0.002	
		0.384	0.553	0.063	
		0.318	0.612	0.070	
		0.272	0.652	0.076	
		0.235	0.686	0.079	
		0.210	0.707	0.083	
		0.189	0.727	0.084	
		0.174	0.738	0.088	
		0.160	0.752	0.088	
		0.153	0.754	0.093	
		0.141	0.766	0.093	
		0.135	0.767	0.098	
		0.041	0.765	0.193	
		0.176	0.741	0.083	
		0.222	0.702	0.076	
		0.244	0.684	0.072	
		0.263	0.668	0.069	
		0.281	0.652	0.067	
		0.297	0.638	0.065	
		0.470	0.048	0.482	
	Top	0.090	0.788	0.122	2.57

	Bottom	0.848	0.144	0.008	
	Top	0.012	0.737	0.251	4.16
	Bottom	0.937	0.058	0.005	
	Top	0.001	0.605	0.394	6.12
	Bottom	0.955	0.041	0.004	
	Top	0.000	0.485	0.515	11.31
	Bottom	0.964	0.033	0.003	
	Top	0.000	0.226	0.774	21.66
	Bottom	0.983	0.015	0.002	
	Critical Point	0.73	0.26	0.01	

Table S 2.5. Absolute deviations between experimental data and NRTL correlated data of the ternary system IL + H_2O + EtOH.

IL	Phase	Experimental data			NRTL correlated data			Absolute Deviation ($\lvert w_{exp}-w_{NRTL}\rvert$)		
		w_{IL}	w_{EtOH}	w_{H2O}	w_{IL}	w_{EtOH}	w_{H2O}	w_{IL}	w_{EtOH}	w_{H2O}
[P_{66614}][Phosph]		0.840	0.000	0.160	0.842	0.000	0.158	0.002	0.000	0.002
	Top	0.356	0.449	0.195	0.363	0.437	0.200	0.007	0.012	0.005
	Bottom	0.053	0.539	0.408	0.059	0.542	0.399	0.006	0.003	0.009
	Top	0.524	0.335	0.141	0.519	0.330	0.151	0.005	0.005	0.010
	Bottom	0.001	0.432	0.567	0.007	0.427	0.567	0.006	0.005	0.000
	Top	0.621	0.255	0.125	0.614	0.259	0.128	0.007	0.004	0.003
	Bottom	0.001	0.317	0.682	0.001	0.313	0.686	0.000	0.005	0.004
	Top	0.718	0.161	0.121	0.718	0.173	0.109	0.000	0.012	0.012
	Bottom	0.000	0.190	0.810	0.000	0.186	0.814	0.000	0.004	0.004
[P_{66614}][Deca]		0.851	0.000	0.149	0.855	0.000	0.146	0.003	0.000	0.003
	Top	0.512	0.341	0.146	0.508	0.335	0.157	0.005	0.006	0.011
	Bottom	0.004	0.429	0.568	0.009	0.424	0.567	0.005	0.005	0.001
	Top	0.615	0.256	0.129	0.610	0.259	0.131	0.005	0.003	0.002
	Bottom	0.000	0.315	0.685	0.001	0.311	0.688	0.001	0.004	0.003
	Top	0.716	0.163	0.122	0.710	0.177	0.113	0.005	0.014	0.009
	Bottom	0.000	0.201	0.799	0.000	0.194	0.806	0.000	0.007	0.007
	Top	0.392	0.419	0.189	0.400	0.409	0.191	0.008	0.010	0.003
	Bottom	0.031	0.509	0.459	0.040	0.510	0.450	0.009	0.001	0.009
[P_{66614}]Cl		0.866	0.000	0.134	0.861	0.001	0.138	0.005	0.001	0.004
	Top	0.438	0.395	0.168	0.429	0.387	0.184	0.008	0.008	0.017
	Bottom	0.079	0.472	0.449	0.058	0.488	0.455	0.021	0.016	0.006
	Top	0.620	0.271	0.109	0.623	0.254	0.123	0.003	0.017	0.014
	Bottom	0.000	0.319	0.681	0.005	0.322	0.674	0.005	0.003	0.007

	Top	0.723	0.175	0.102	0.729	0.170	0.101	0.006	0.005	0.001
	Bottom	0.000	0.198	0.802	0.000	0.202	0.798	0.000	0.004	0.004
	Top	0.807	0.082	0.111	0.815	0.091	0.094	0.007	0.009	0.017
	Bottom	0.000	0.100	0.900	0.000	0.099	0.901	0.000	0.002	0.001
$[P_{66614}][CH_3SO_3]$		0.872	0.000	0.128	0.881	0.000	0.119	0.009	0.000	0.009
	Top	0.590	0.257	0.153	0.597	0.245	0.158	0.007	0.013	0.005
	Bottom	0.031	0.306	0.663	0.034	0.311	0.655	0.002	0.005	0.008
	Top	0.703	0.176	0.121	0.695	0.171	0.135	0.008	0.005	0.013
	Bottom	0.006	0.218	0.776	0.019	0.208	0.774	0.012	0.010	0.002
	Top	0.510	0.305	0.185	0.504	0.308	0.188	0.006	0.003	0.003
	Bottom	0.088	0.381	0.531	0.067	0.395	0.538	0.021	0.014	0.007
	Top	0.795	0.085	0.120	0.798	0.083	0.119	0.002	0.002	0.001
	Bottom	0.003	0.092	0.905	0.013	0.093	0.894	0.009	0.001	0.010
$[P_{66614}]Br$		0.937	0.000	0.063	0.934	0.000	0.066	0.003	0.000	0.003
	Top	0.054	0.555	0.391	0.047	0.555	0.398	0.007	0.000	0.007
	Bottom	0.562	0.348	0.090	0.551	0.346	0.103	0.012	0.002	0.013
	Top	0.645	0.280	0.075	0.649	0.273	0.078	0.004	0.007	0.003
	Bottom	0.010	0.436	0.554	0.007	0.440	0.553	0.003	0.004	0.001
	Top	0.128	0.572	0.300	0.129	0.579	0.292	0.000	0.007	0.008
	Bottom	0.449	0.426	0.126	0.451	0.418	0.132	0.002	0.008	0.006
	Top	0.718	0.223	0.059	0.718	0.220	0.062	0.000	0.003	0.003
	Bottom	0.001	0.326	0.673	0.001	0.326	0.673	0.000	0.001	0.000
$[P_{66614}][N(CN)_2]$		0.967	0.000	0.033	0.978	0.009	0.013	0.011	0.009	0.021
	Top	0.622	0.313	0.065	0.623	0.311	0.067	0.001	0.003	0.002
	Bottom	0.020	0.574	0.406	0.021	0.574	0.405	0.001	0.000	0.001
	Top	0.712	0.238	0.050	0.689	0.256	0.054	0.023	0.018	0.005
	Bottom	0.009	0.463	0.528	0.003	0.457	0.539	0.006	0.006	0.011
	Top	0.434	0.458	0.108	0.462	0.437	0.102	0.028	0.021	0.006
	Bottom	0.115	0.634	0.252	0.144	0.626	0.230	0.029	0.008	0.022
	Top	0.787	0.169	0.044	0.753	0.204	0.043	0.034	0.035	0.001
	Bottom	0.009	0.330	0.662	0.000	0.318	0.681	0.008	0.011	0.020
$[P_{66614}][NTf_2]$		0.998	0.000	0.002	0.999	0.000	0.001	0.001	0.000	0.001
	Top	0.012	0.737	0.252	0.049	0.697	0.254	0.037	0.039	0.002
	Bottom	0.937	0.058	0.005	0.903	0.090	0.007	0.034	0.032	0.002
	Top	0.090	0.789	0.122	0.152	0.735	0.114	0.062	0.054	0.008
	Bottom	0.848	0.144	0.009	0.864	0.128	0.008	0.017	0.016	0.001
	Top	0.000	0.485	0.515	0.005	0.480	0.515	0.005	0.005	0.000
	Bottom	0.964	0.033	0.003	0.930	0.065	0.005	0.035	0.032	0.002
	Top	0.001	0.605	0.394	0.015	0.593	0.392	0.014	0.012	0.002

Bottom	0.955	0.041	0.004	0.920	0.074	0.006	0.035	0.033	0.002
Top	0.000	0.226	0.774	0.000	0.222	0.778	0.000	0.004	0.004
Bottom	0.983	0.015	0.002	0.954	0.043	0.003	0.029	0.028	0.001

COMPARISON BETWEEN ALL EXPERIMENTAL TERNARY PHASE DIAGRAMS

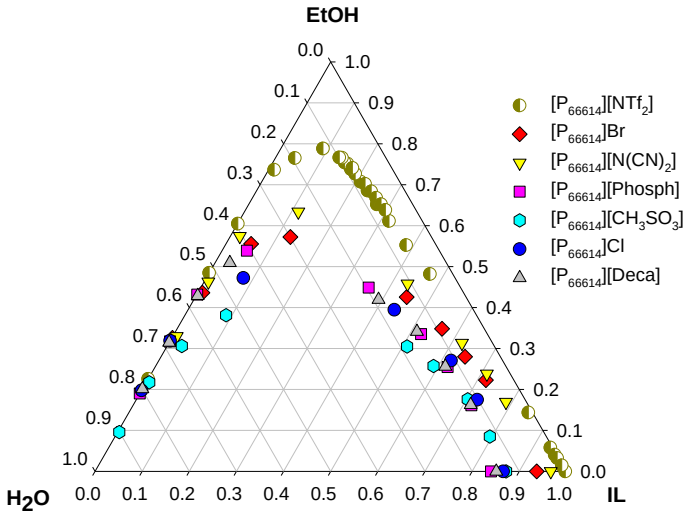

Figure S 2.7. Experimental ternary phase diagrams for all IL + EtOH + H_2O systems at 298.15 K (mass fraction units).

CONSISTENCY OF THE EXPERIMENTAL TIE-LINES

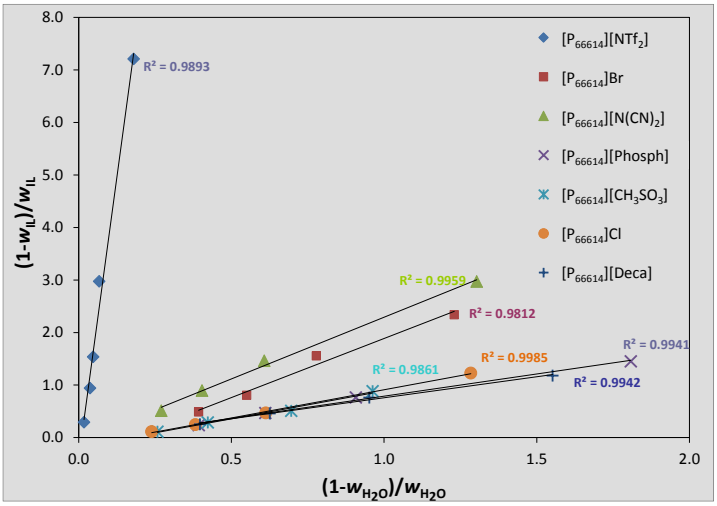

Figure S 2.8. Tie-Lines correlation using the Othmer-Tobias correlation[2] for each ternary system IL + EtOH + Water.

S AND *D* DEPENDENCE ON THE ETHANOL CONTENT

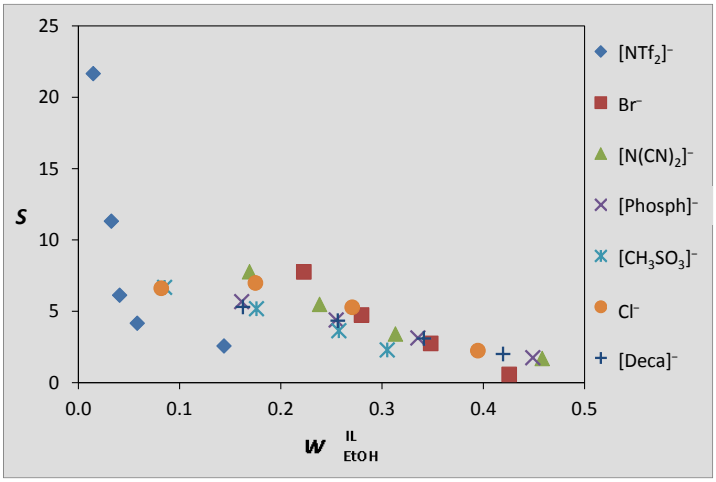

Figure S 2.9. Correlation of ethanol selectivities (*S*) as a function of the ethanol content in the IL-rich phase (w_{EtOH}^{IL}).

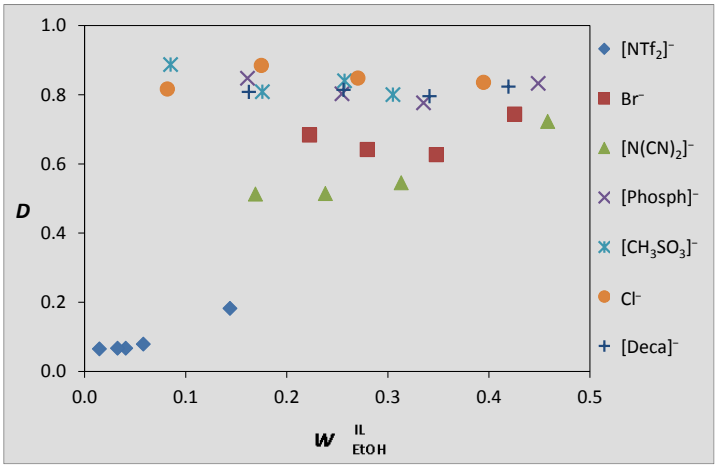

Figure S 2.10. Correlation of ethanol distribution coefficients (*D*) as a function of the ethanol content in the IL-rich phase (w_{EtOH}^{IL}).

NRTL PARAMETER ESTIMATION

The expressions for the excess Gibbs energy (g^E) and the logarithm of the activity coefficient ($\ln \gamma_i$) given by the NRTL model can be written as:[3]

$$\frac{g^E}{RT} = \sum_i^{n_c} x_i \ln \gamma_i = \sum_i^{n_c} \frac{x_i L_i}{M_i} \tag{S2.1}$$

$$\ln \gamma_i = \frac{L_i}{M_i} + \sum_j^{n_c} \frac{x_j G_{ij}}{M_j} (\tau_{ij} - \frac{L_j}{M_j}) \tag{S2.2}$$

$$L_i = \sum_k^{n_c} x_k \tau_{ki} G_{ki} \tag{S2.3}$$

$$M_i = \sum_k^{n_c} x_k G_{ki} \tag{S2.4}$$

$$G_{ij} = e^{-\alpha_{ij}\tau_{ij}} \tag{S2.5}$$

$$\tau_{ij} = \frac{(g_{ij} - g_{ii})}{RT} = \frac{\Delta g_{ij}}{RT},\ i \neq j \text{ and } \tau_{ij} = 0,\ i = j \tag{S2.6}$$

Here $i, j, k \in \{1,2,3\}$ represent the different molecular species in the mixture (1 – water, 2 – ethanol, 3 – ionic liquid), n_c is the number of components, and x_i refers to molar fractions. In the present work, the parameter estimation task was formulated as the solution of a nonlinear programming problem (NLP), using the weighted norm of the differences between the experimental mass fractions and the values predicted by the model as an objective function:[4]

$$\min_z \ \phi = \sum_i^{n_t} \sum_j^{n_c} \sum_k^{2} \omega_{ijk} e_{ijk}(\tau)^2 \tag{S2.7}$$

where $e_{ijk}(\tau) = w_{ijk}^{\exp} - w_{ijk}^{\mathrm{mod}}(\tau)$, and the superscripts *exp* and *mod* correspond to experimental and predicted mass fraction values, respectively. The summations in this equation are taken over all tie-lines (i), components (j) and phases (k), and ω_{ijk} is a weight factor associated with each error term. Using the isothermal data available for each system, the objective function ϕ was minimized by simultaneous determination of all model variables (here denoted as z), subject to constraints of iso-activity, the NRTL

activity model described by equations (S2-S6), sum of mass and molar fraction restrictions, and magnitude bounds for the model parameters τ_{ij}. Mass fractions were used in the data regression, due to the large differences in molecular weights between the ionic liquids and the molecular components.

To address the non-convexity of this nonlinear parameter estimation problem, which often leads to multiple local optimal solutions, this problem was implemented in GAMS,[5] taking advantage of the robustness of the numerical solvers available in this system. Additionally, considerable care was placed in the reformulation of the original model equations, as NLP constraints. This was done by introducing new terms and using algebraic rearrangements in the resultant equations that allowed the nonlinearity of each individual component of the model to be significantly decreased. Scaling of the resulting variables and equations was performed, also with the purpose of reducing the overall model nonlinearity. A subset of fundamental model variables was identified, and proper initialization and bounds were established for them. These values were then propagated throughout the model to initialize and bound the remaining variables, allowing both a more consistent global model initialization, and avoiding the nonconvergence of the NLP due to the inability of locating feasible solutions. This step was verified to be an essential task to guarantee the convergence of the parameter estimation. The following numerical solvers were used in this study:

CONOPT[6] – based on the General Reduced Gradient and Successive Quadratic Programming algorithms; provides a very robust initialization and location of feasible points in highly constrained problems; suitable for medium to large scale NLPs;

OQNLP[7] – a global solver based on various heuristic multistart algorithms; designated to rapidly finding various local optima of smooth constrained NLPs;

BARON[8] – a global numerical solver for continuous and discrete variables; based on a deterministic global optimization algorithm; capable of determining and refining model bounds in different regions of the solution domain.

Each of these solvers was tested with each LLE ternary system, to ensure that the set of parameters obtained corresponds to the best possible solutions using this type of formulation. The values of the residual function ϕ at the optimum were comprised between 0.7×10^{-3} (system with Br^-) and 7×10^{-3} (for the system with $[N(CN)_2]^-$). This was possible through the extensive search for alternative solutions (especially with the OQNLP solver) and by increasing the bounds allowed for the τ_{ij} parameters, which in various cases resulted in higher values for the interaction parameter τ_{13} (water – ionic liquid). This step should be interpreted with caution, since it corresponds to larger values of the respective Δg_{ij} interaction term, and would perhaps benefit from additional confirmation provided by including in the regression experimental data obtained at different temperatures.

The computer requirements for the parameter estimation task were of the order of one second of CPU, using GAMS/CONOPT on a current Intel Xeon Linux workstation. Due to different nature of the algorithms, a maximum of 30 minutes of CPU were allowed for the runs with the OQNLP solver, and 60 minutes for BARON. Within the time allowed and for all the systems considered, BARON was unable to find a guaranteed global solution, stopping often at a local solution. On the other hand, the OQNLP solver was able to identify several distinct local solutions of the problems. This number of local optima found varied from 5 (for the system with $[NTf_2]^-$) to 77 (system with Br^-), and corresponded typically to approximately 20 different local optima, in most of the cases considered. Within this set, the solutions provided by CONOPT corresponded typically to the best (or second best) local solutions known for each problem, after reasonable tuning of the initialization scheme. From an overall perspective, the experience acquired in this part of the work indicates that the critical steps in this parameter estimation task were the proper construction of the NLP (through reformulation, scaling, initialization and bounding of the original mathematical model), and the availability of a multistart optimizer, capable of largely eliminating the effects of the initial estimates on the quality of the solutions obtained.

Appendix Chapter 3 – Mutual Solubilities of Ionic Liquids and Water

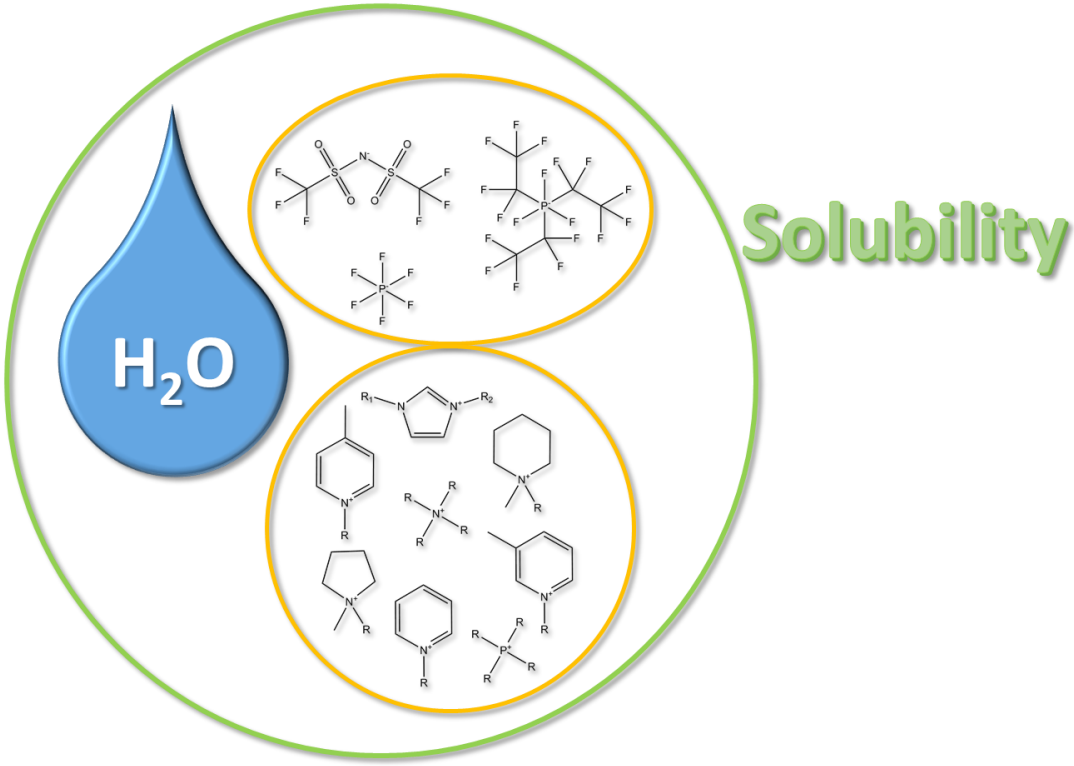

3.4. Thermophysical properties and water saturation of [PF_6]-based ionic liquids

Catarina M. S. S. Neves, Marta L. S. Batista, Ana Filipa M. Cláudio, Luís M. N. B. F. Santos, Isabel M. Marrucho, Mara G. Freire and João A. P. Coutinho, Journal of Chemical & Engineering Data 55 (2010) 5065-5073, DOI: 10.1021/je100638g

DSC THERMOGRAMS

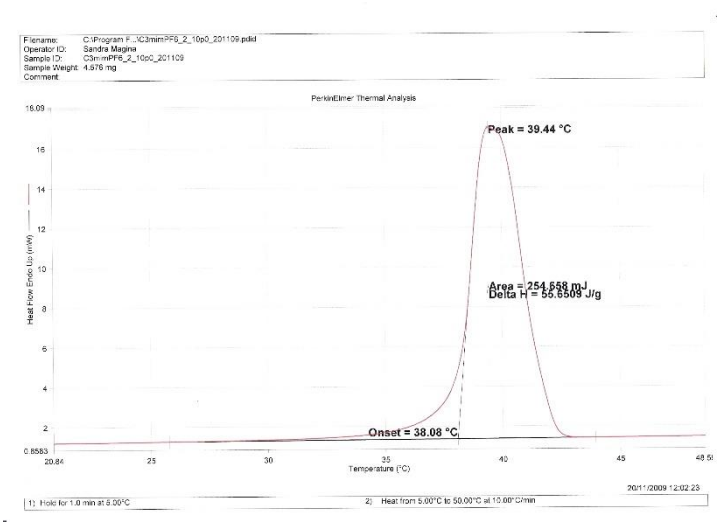

Figure S 3.1. Thermogram for [C_3C_1im][PF_6] obtained using a Diamond DSC PerkinElmer equipment.

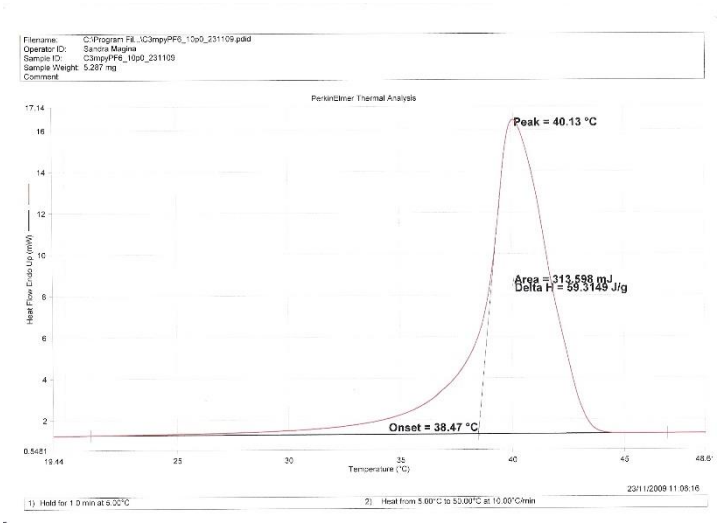

Figure S 3.2. Thermogram for [C_3-3-C_1py][PF_6] obtained using a Diamond DSC PerkinElmer equipment.

MUTUAL SOLUBILITIES MEASUREMENTS

Calibration curves for the ionic liquids solubility in water determination were achieved using a stock solution of each ionic liquid in ultra-pure water with a concentration of ≈ 0.5 $g \cdot dm^{-3}$. Proper dilutions in ultra-pure water of the stock solution guided to nine standard solutions. The concentration of each standard is given in Table S3.3, and the calibration curves are given in Figure S3.1. The absorbance of each standard solution is an average of at least 5 independent readings.

Table S 3.1. Concentration of the stock solution and respective standard solutions of each IL, as well as respective absorbance at λ = 211 nm or 266 nm.

	$[C_3C_1im][PF_6]$		$[C_3\text{-}3\text{-}C_1py][PF_6]$	
Stock Solution / $g \cdot dm^{-3}$	0.4424		0.4884	
Standard Solutions	[IL] / $g \cdot dm^{-3}$	Absorbance at λ = 211 nm	[IL] / $g \cdot dm^{-3}$	Absorbance at λ = 266 nm
1	0.0044	0.072	0.0146	0.251
2	0.0088	0.150	0.0195	0.329
3	0.0133	0.210	0.0244	0.415
4	0.0177	0.284	0.0293	0.494
5	0.0265	0.426	0.0342	0.577
6	0.0354	0.550	0.0391	0.661
7	0.0442	0.686	0.0440	0.747
8	0.0531	0.829	0.0488	0.836
9	0.0619	0.967	0.0733	1.243

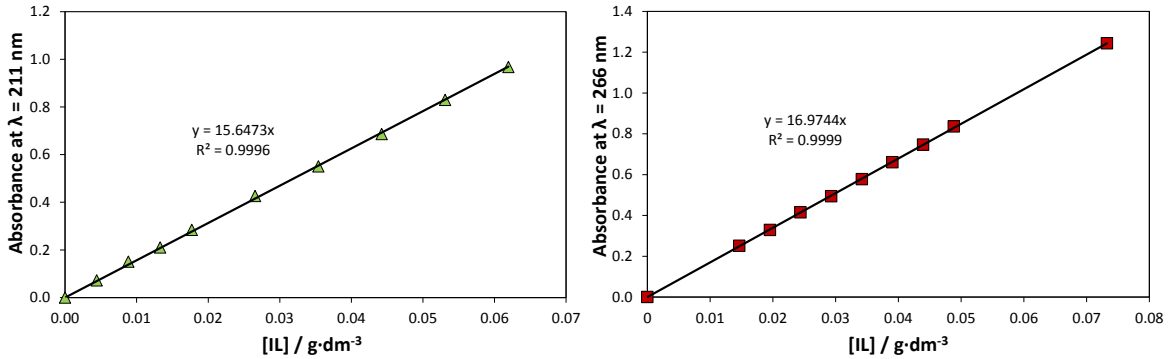

Figure S 3.3. Calibration Curves (Absorbance at λ = 211 nm or 266 nm as a function of the IL concentration) for ILs: ▲, $[C_3C_1im][PF_6]$; ■, $[C_3\text{-}3\text{-}C_1py][PF_6]$.

Table S 3.2. Experimental mole fraction solubility of water in ILs, x_w, and of ILs in water, x_{IL}, as a function of temperature and at 0.1 MPa.

	$x_w \pm \sigma$[a]		10^3 ($x_{IL} \pm \sigma$[a])	
T / K	$[C_3C_1im][PF_6]$	$[C_3\text{-}3C_1py][PF_6]$	$[C_3C_1im][PF_6]$	$[C_3\text{-}3\text{-}C_1py][PF_6]$
288.15	0.2437 ± 0.0016	---	1.158 ± 0.040	0.918 ± 0.050
293.15	0.2709 ± 0.0009	---	1.543 ± 0.008	1.223 ± 0.024
298.15	0.2925 ± 0.0009	---	1.957 ± 0.011	1.646 ± 0.029
303.15	0.3168 ± 0.0025	0.2949 ± 0.0020	2.528 ± 0.012	1.990 ± 0.002
308.15	0.3461 ± 0.0003	0.3248 ± 0.0008	2.772 ± 0.066	2.204 ± 0.028
313.15	0.3769 ± 0.0029	0.3516 ± 0.0035	2.965 ± 0.021	2.363 ± 0.020
318.15	0.4050 ± 0.0017	0.3772 ± 0.0025	3.314 ± 0.015	2.689 ± 0.027

[a]Standard deviation

Table S 3.3. Correlation parameters for the mole fraction solubility of water in ILs and ILs in water as a function of temperature using eqs 3.1 and 3.2, respectively.

IL	A	B / K	R^2 [(a)]	C [(b)]	D / K [(b)]	E [(b)]	R^2 [(a)]
$[C_3C_1im][PF_6]$	3.94 ± 0.15	-1541 ± 44	0.9990	-315 ± 405	12816 ± 18676	47 ± 60	0.9969
$[C_3\text{-}3\text{-}C_1py][PF_6]$	3.99 ± 0.44	-1579 ± 180	0.9965	-425 ± 537	17712 ± 24742	63 ± 80	0.9955

[(a)] Correlation coefficient.

[(b)] Note that three correlation constants were calculated from four experimental data points [from (303.15 to 318.15) K] to avoid discrepancies between liquid-liquid and solid-liquid equilibria.

DENSITY

Table S 3.4. Experimental density values, ρ, for pure ILs and (IL + water) systems as a function of temperature and at 0.1 MPa, where x_w is the constant mole fraction solubility of water in the IL at $T \approx 300$ K.

	ρ / kg·m^{-3}			
	$[C_3C_1im][PF_6]$	$[C_3\text{-}3\text{-}C_1py][PF_6]$	$[C_3C_1im][PF_6]$	$[C_3\text{-}3\text{-}C_1py][PF_6]$
T / K	Pure		x_w = (0.306 ± 0.004[a])	x_w = (0.249 ± 0.006[a])
303.15	---	---	1389.2	1362.5
308.15	---	---	1384.7	1358.3
313.15	---	---	1380.2	1354.0
318.15	1397.5	1365.4	1375.7	1349.8
323.15	1393.2	1361.3	1371.3	1345.6
328.15	1389.0	1357.3	1366.9	1341.4
333.15	1384.7	1353.2	1362.5	1337.2
338.15	1380.5	1349.2	1358.1	1333.1
343.15	1376.3	1345.2	1353.8	1328.9
348.15	1372.1	1341.2	1349.4	1324.8
353.15	1367.9	1337.2	1345.1	1320.7

358.15	1363.8	1333.2	1340.8	1316.6
363.15	1359.6	1329.2	1336.5	1312.5

[a]Standard deviation

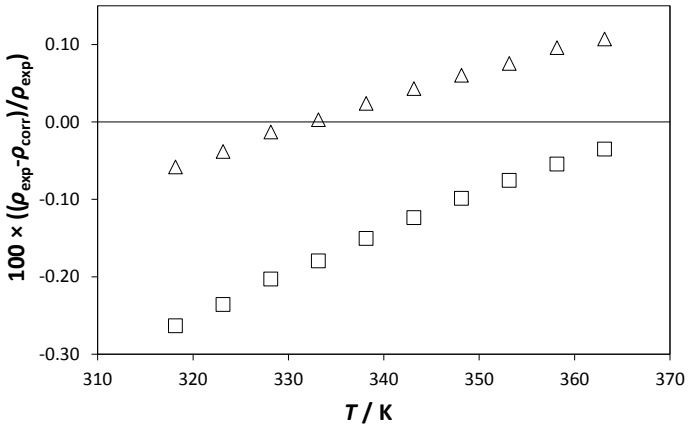

Figure S 3.4. Density deviation plot between measured data and predicted values using eq 3.6: △, $[C_3C_1im][PF_6]$; □, $[C_3\text{-}3\text{-}C_1py][PF_6]$.

VISCOSITY

Table S 3.5. Experimental viscosity values, η, for pure ILs and (IL + water) systems as a function of temperature and at 0.1 MPa, where x_w is the constant mole fraction solubility of water in the IL at $T \approx 300$ K.

	η / mPa·s			
	$[C_3C_1im][PF_6]$	$[C_3\text{-}3\text{-}C_1py][PF_6]$	$[C_3C_1im][PF_6]$	$[C_3\text{-}3\text{-}C_1py][PF_6]$
T / K	Dried		x_w = (0.306 ± 0.004 [a])	x_w = (0.249 ± 0.006 [a])
303.15	---	---	39.408	73.388
308.15	---	---	32.254	57.548
313.15	---	---	26.844	45.980
318.15	85.006	132.870	22.612	37.356
323.15	68.178	102.170	19.285	30.806
328.15	55.458	79.968	16.581	25.755
333.15	45.700	63.669	14.386	21.759
338.15	38.092	51.520	12.612	18.602
343.15	32.099	42.287	11.134	16.037
348.15	27.321	35.160	9.905	13.976
353.15	23.469	29.579	8.874	12.277
358.15	20.337	25.148	7.983	10.861
363.15	17.771	21.594	7.228	9.677

[a]Standard deviation

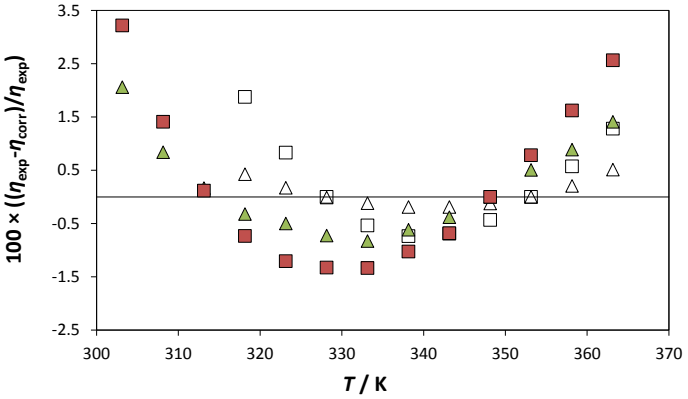

Figure S 3.5. Viscosity deviation plot between measured data and predicted values using eqs 3.8 to 3.10 for pure (empty symbols) and water-saturated (full symbols) ILs: △, ▲, [C_3C_1im][PF_6]; □, ■, [C_3-3-C_1py][PF_6].

3.5. Mutual solubility of water and structural/positional isomers of N-alkylpyridinium-based ionic liquids

Mara G. Freire, Catarina M. S. S. Neves, Karina Shimizu, Carlos E. S. Bernardes, Isabel M. Marrucho, João A. P. Coutinho, José N. Canongia Lopes and Luís Paulo N. Rebelo, Journal of Physical Chemistry B 114 (2010) 15925-15934, DOI: 10.1021/jp1093788

NMR SPECTRA

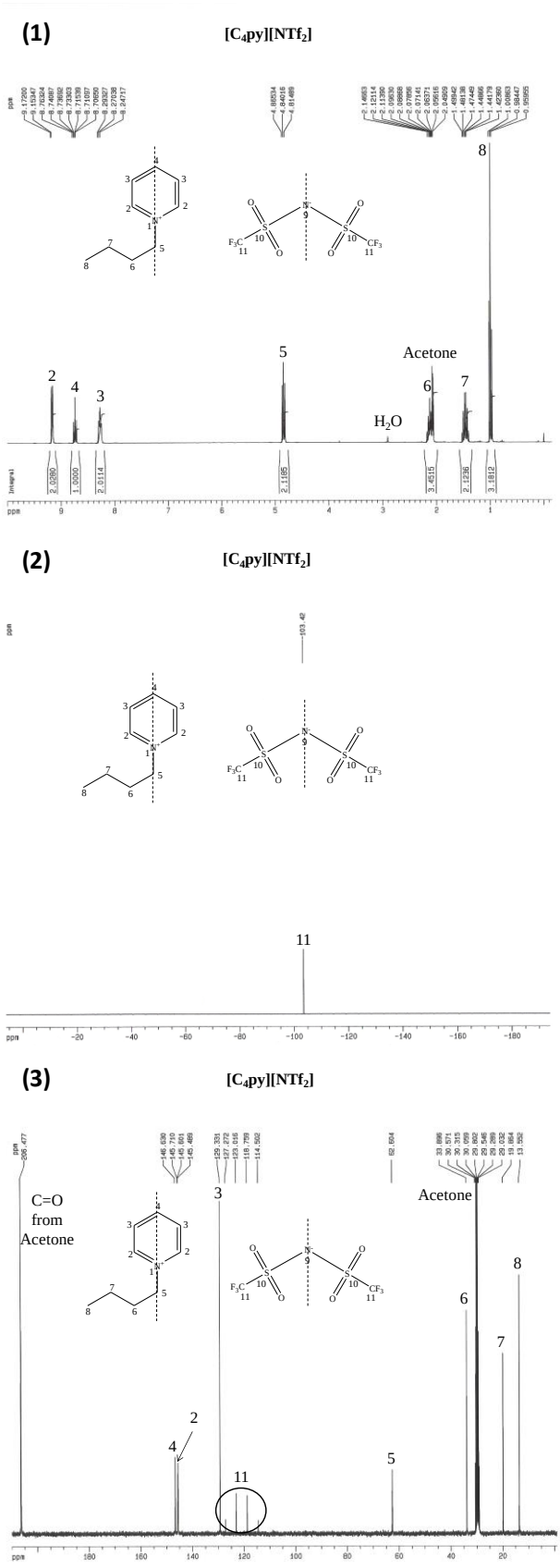

Figure S 3.6. ^{1}H (1), ^{19}F (2), ^{13}C (3) NMR spectra of [C4py][NTf2] in CD_3COCD_3.

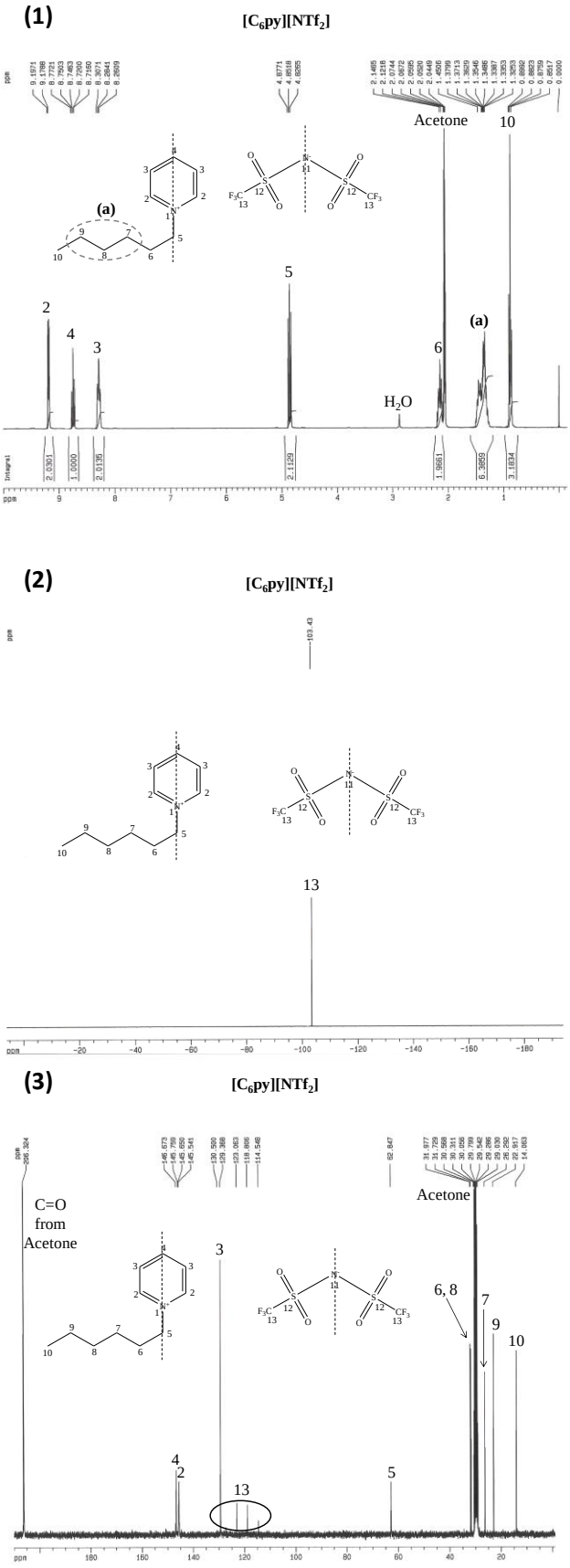

Figure S 3.7. ^{1}H (1), ^{19}F (2), ^{13}C (3) NMR spectra of $[C_6py][NTf_2]$ in CD_3COCD_3.

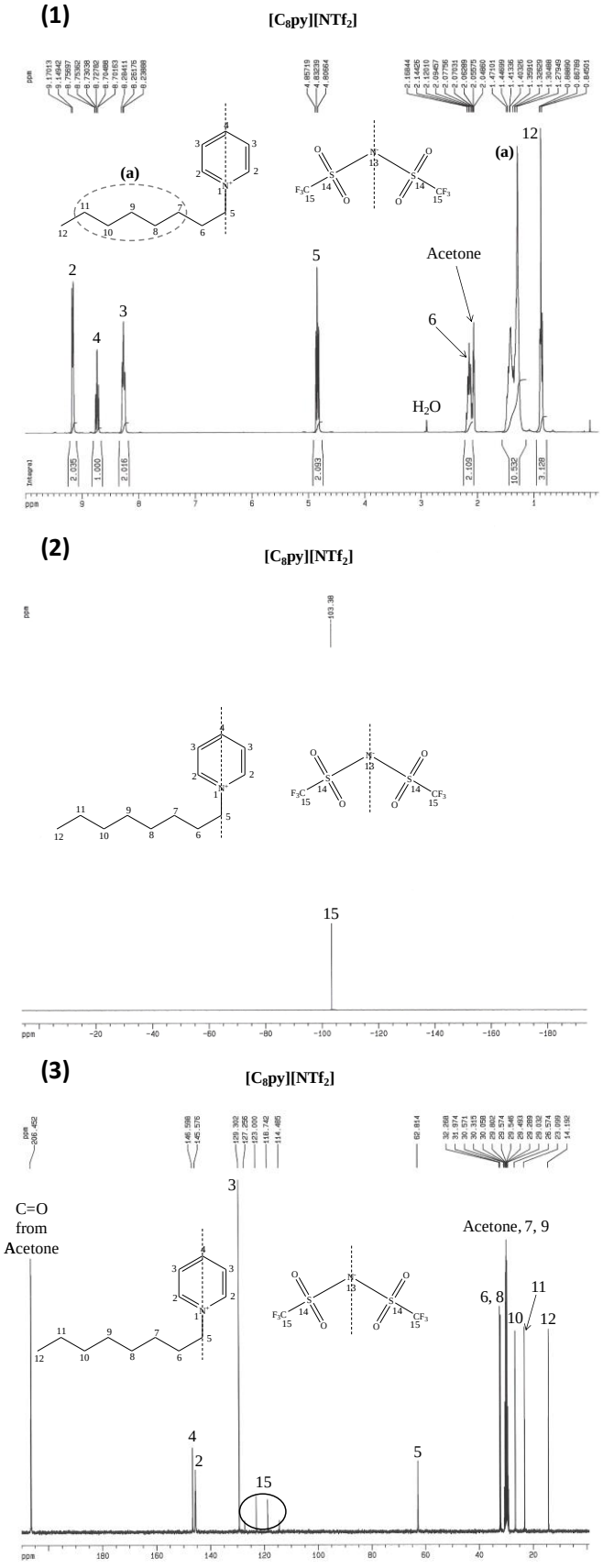

Figure S 3.8. ^{1}H (1), ^{19}F (2), ^{13}C (3) NMR spectra of $[C_8py][NTf_2]$ in CD_3COCD_3.

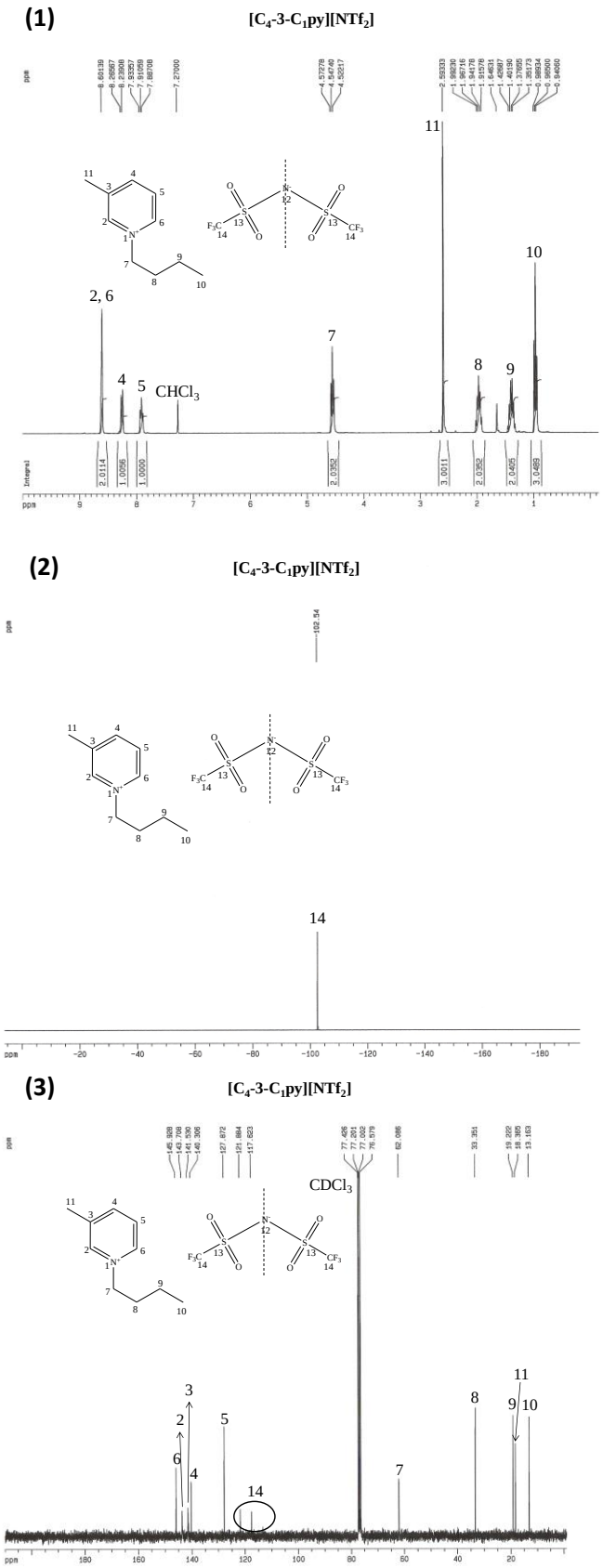

Figure S 3.9. ^{1}H (1), ^{19}F (2), ^{13}C (3) NMR spectra of $[C_4\text{-}3\text{-}C_1py][NTf_2]$ in CD_3COCD_3.

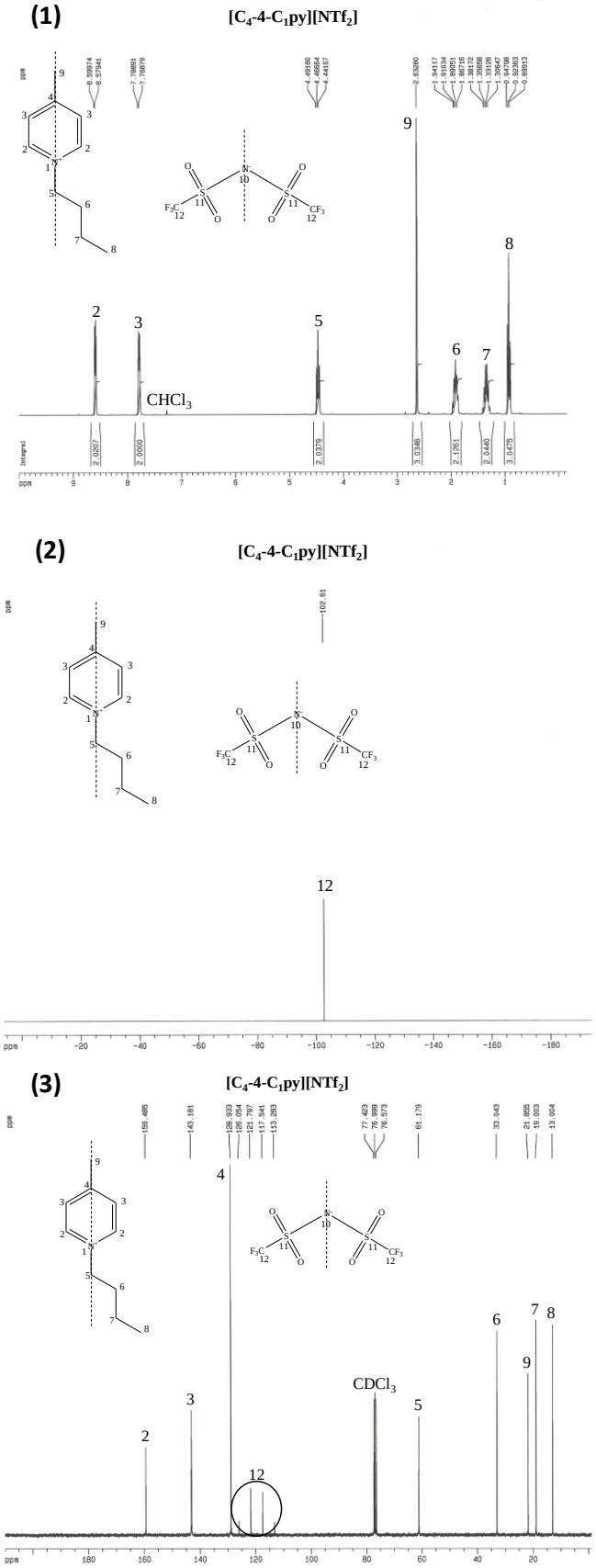

Figure S 3.10. ^{1}H (1), ^{19}F (2), ^{13}C (3) NMR spectra of $[C_4\text{-}4\text{-}C_1py][NTf_2]$ in CD_3COCD_3.

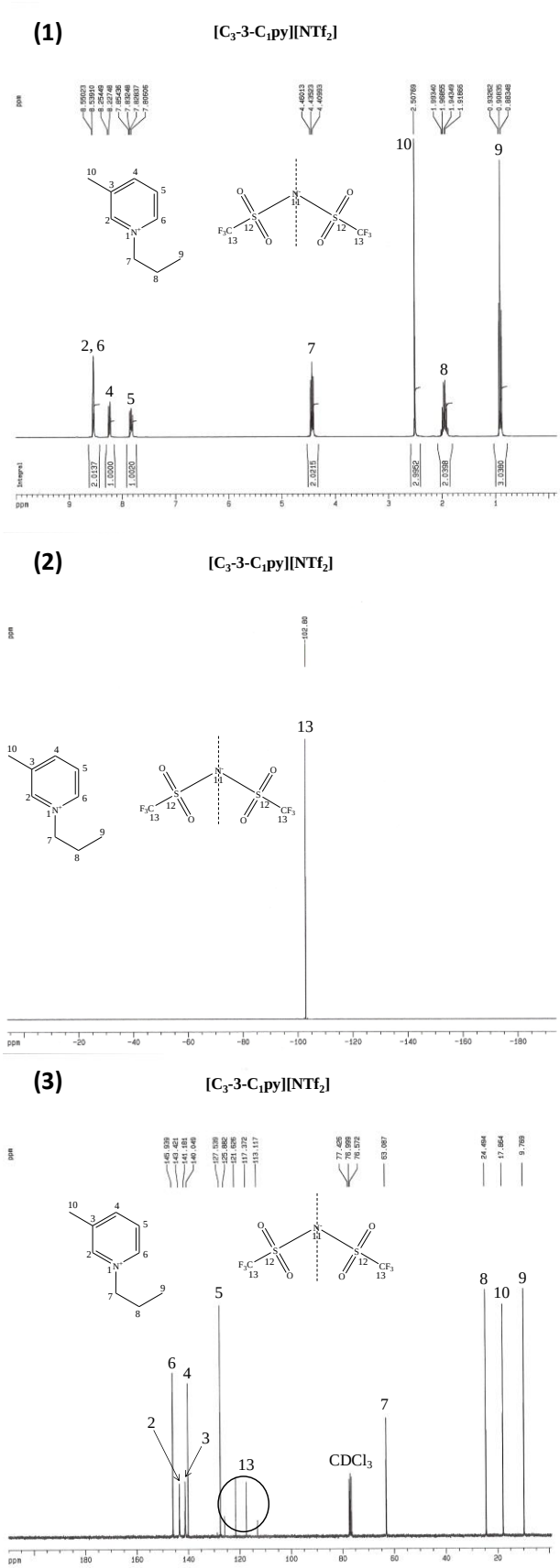

Figure S 3.11. ^{1}H (1), ^{19}F (2), ^{13}C (3) NMR spectra of $[C_3\text{-}3\text{-}C_1py][NTf_2]$ in CD_3COCD_3.

MUTUAL SOLUBILITIES MEASUREMENTS

Table S 3.6. Solubilities of water in the IL-rich phase (expressed in water mole fraction, x_w) and of IL in the water-rich phase (expressed in IL mole fraction, x_{IL}) at different temperatures, and respective deviations.

	[C4py][NTf2]	[C6py][NTf2]	[C8py][NTf2]	[C4-3-C1py][NTf2]	[C4-4-C1py][NTf2]
T/K			x_w		
288.15	0.221 ± 0.003	0.204 ± 0.002	0.175 ± 0.003	0.190 ± 0.002	0.219 ± 0.001
293.15	0.238 ± 0.001	0.216 ± 0.001	0.188 ± 0.010	0.202 ± 0.001	0.234 ± 0.003
298.15	0.252 ± 0.001	0.225 ± 0.002	0.197 ± 0.010	0.213 ± 0.001	0.247 ± 0.003
303.15	0.269 ± 0.003	0.246 ± 0.003	0.216 ± 0.060	0.232 ± 0.002	0.264 ± 0.002
308.15	0.291 ± 0.001	0.260 ± 0.001	0.234 ± 0.030	0.248 ± 0.001	0.285 ± 0.003
313.15	0.309 ± 0.003	0.277 ± 0.005	0.250 ± 0.010	0.261 ± 0.003	0.302 ± 0.002
318.15	0.327 ± 0.003	0.294 ± 0.001	0.267 ± 0.020	0.277 ± 0.001	0.319 ± 0.001
T/K			$10^4 \cdot x_{IL}$		
288.15	3.31 ± 0.02	1.85 ± 0.01	0. 309 ± 0.001	1.99 ± 0.01	2.06 ± 0.02
293.15	3.39 ± 0.03	1.96 ± 0.02	0.337 ± 0.003	2.06 ± 0.01	2.12 ± 0.03
298.15	3.55 ± 0.05	2.00 ± 0.01	0.350 ± 0.003	2.10 ± 0.04	2.21 ± 0.06
303.15	3.73 ± 0.02	2.07 ± 0.05	0.389 ± 0.04	2.18 ± 0.04	2.38 ± 0.03
308.15	3.98 ± 0.02	2.26 ± 0.08	0.420 ± 0.002	2.30 ± 0.05	2.52 ± 0.07
313.15	4.11 ± 0.01	2.43 ± 0.09	0.446 ± 0.007	2.44 ± 0.02	2.62 ± 0.08
318.15	4.53 ± 0.03	2.56 ± 0.06	0.507 ± 0.009	2.54 ± 0.02	2.82 ± 0.07

Table S 3.7. Weight fraction solubility of water in the IL-rich phase (w_w) and weigth fraction solubility of IL in the water-rich Phase (w_{IL}) at different temperatures

	[C4py][NTf2]	[C6py][NTf2]	[C8py][NTf2]	[C4-3-C1py][NTf2]	[C4-4-C1py][NTf2]
T / K			$100(w_w \pm \sigma^a)$		
288.15	1.212 ± 0.014	1.029 ± 0.007	0.804 ± 0.012	0.970 ± 0.009	1.159 ± 0.004
293.15	1.334 ± 0.004	1.107 ± 0.004	0.873 ± 0.005	1.049 ± 0.004	1.262 ± 0.013
298.15	1.435 ± 0.005	1.165 ± 0.007	0.927 ± 0.003	1.119 ± 0.006	1.353 ± 0.014
303.15	1.571 ± 0.015	1.307 ± 0.011	1.037 ± 0.022	1.248 ± 0.009	1.479 ± 0.010
308.15	1.741 ± 0.005	1.408 ± 0.003	1.153 ± 0.010	1.362 ± 0.005	1.643 ± 0.011
313.15	1.896 ± 0.011	1.528 ± 0.020	1.252 ± 0.003	1.460 ± 0.014	1.776 ± 0.010
318.15	2.056 ± 0.011	1.659 ± 0.004	1.369 ± 0.008	1.579 ± 0.001	1.919 ± 0.005
T / K			$100(w_{IL} \pm \sigma^a)$		
288.15	0.760 ± 0.004	0.454 ± 0.001	0.0810 ± 0.0026	0.473 ± 0.002	0.490 ± 0.006
293.15	0.778 ± 0.006	0.481 ± 0.005	0.0883 ± 0.0007	0.489 ± 0.003	0.505 ± 0.008
298.15	0.815 ± 0.011	0.491 ± 0.001	0.0917 ± 0.0008	0.500 ± 0.010	0.526 ± 0.015
303.15	0.855 ± 0.004	0.508 ± 0.012	0.1018 ± 0.0010	0.518 ± 0.009	0.565 ± 0.008
308.15	0.911 ± 0.004	0.554 ± 0.019	0.1102 ± 0.0005	0.546 ± 0.012	0.598 ± 0.016

313.15	0.942 ± 0.002	0.596 ± 0.022	0.1168 ± 0.0019	0.579 ± 0.004	0.623 ± 0.018
318.15	1.036 ± 0.006	0.628 ± 0.015	0.1328 ± 0.0046	0.604 ± 0.006	0.670 ± 0.018

[a]Standard Deviation

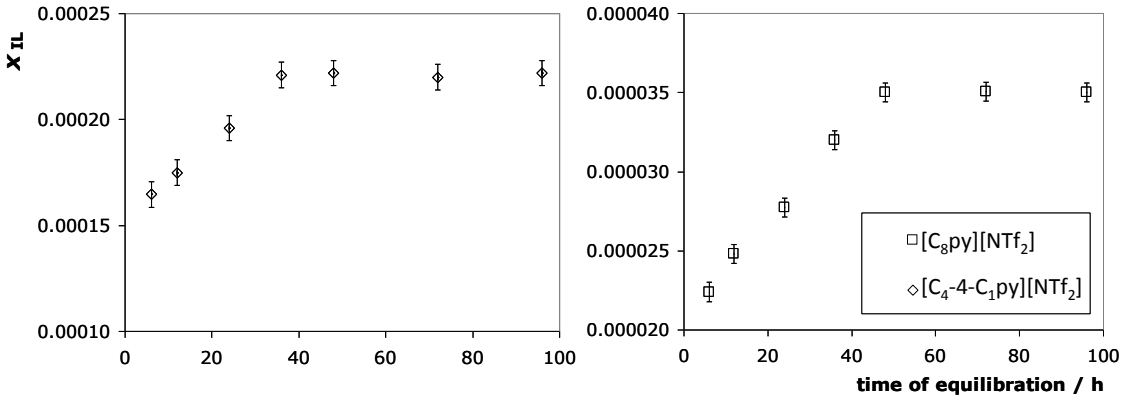

Figure S 3.12. Solubility of [C_4-4-C_1py][NTf_2] and [C_8py][NTf_2] *versus* time of equilibration at 298.15 K.

3.6. Solubility of non-aromatic hexafluorophosphate-based salts and ionic liquids in water determined by electrical conductivity

Catarina M. S. S. Neves, Ana R. Rodrigues, Kiki A. Kurnia, José M. S. S. Esperança, Mara G. Freire and João A. P. Coutinho, Fluid Phase Equilibria 358 (2013) 50-55, DOI: 10.1016/j.fluid.2013.07.061

SOLUBILITY OF HEXAFLUOROPHOSPHATE-BASED SALTS IN WATER

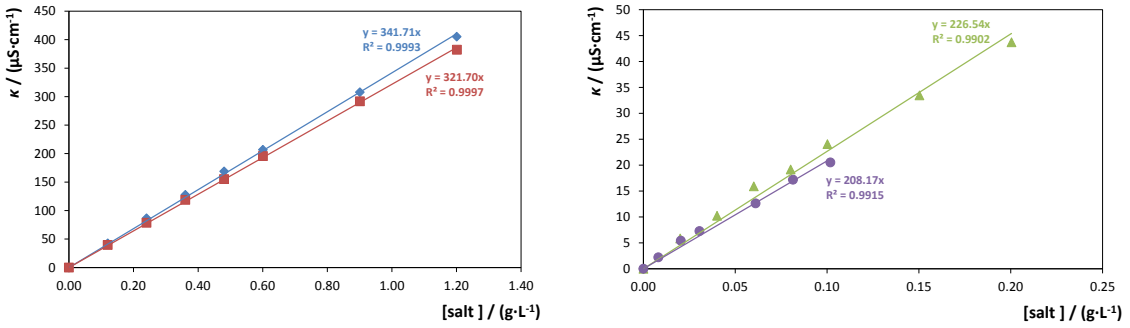

Figure S 3.13. Calibration curves for (◆) [C_3C_1pyr][PF_6], (■) [C_3C_1pip][PF_6], (▲) [N_{4444}][PF_6] and (●) [P_{4444}][PF_6].

Table S 3.8. Experimental mole fraction solubilities (x_{salt}) and respective uncertainty ($2u(x_{salt})$) of the [PF_6]-based salts in water, as function of temperature and at 0.1 MPa.

T / K	[C_4C_1im][PF_6]	[C_3C_1pyr][PF_6]	[C_3C_1pip][PF_6]	[N_{4444}][PF_6]	[P_{4444}][PF_6]
		10^3 (x_{salt} ± 2u(x_{salt})[a])		10^5 (x_{salt} ± 2u(x_{salt})[a])	
288.15	1.08 ± 0.02	1.28 ± 0.02	0.936 ± 0.004	2.24 ± 0.26	1.71 ± 0.16
293.15	1.15 ± 0.02	1.36 ± 0.02	0.985 ± 0.012	2.43 ± 0.04	1.80 ± 0.02
298.15	1.22 ± 0.02	1.57 ± 0.06	1.090 ± 0.008	2.60 ± 0.22	1.85 ± 0.06
303.15	1.41 ± 0.04	1.82 ± 0.02	1.337 ± 0.006	2.82 ± 0.20	1.94 ± 0.04
308.15	1.61 ± 0.02	2.19 ± 0.04	1.562 ± 0.016	3.07 ± 0.10	2.11 ± 0.24
313.15	1.77 ± 0.02	2.81 ± 0.02	1.787 ± 0.016	3.26 ± 0.24	2.24 ± 0.08
318.15	2.02 ± 0.02	3.10 ± 0.04	2.133 ± 0.024	3.40 ± 0.16	2.38 ± 0.14

[a] Expanded uncertainty at the 0.95 confidence level, $2u(x_{salt})$, evaluated from the standard deviation and applying a coverage factor $k = 2$.

COSMO-RS

Table S 3.9. Predicted solubility of the [PF_6]-based salts in water using COSMO-RS and the different contributions from their enthalpies of phase transition.

Salt	T/K	ΔH_{fus}/ (kJ·mol^{-1})	($\Delta H_{fus} + \Delta H_{T,2}$)/ (kJ·mol^{-1})	($\Delta H_{fus} + \Delta H_{T,1} + \Delta H_{T,2}$)/ (kJ·mol^{-1})
		lnx_{salt}	lnx_{salt}	lnx_{salt}
[C_3C_1pyr][PF_6]	288.15	-4.48	-4.72	-5.01
	293.15	-4.44	-4.66	-4.93
	298.15	-4.40	-4.60	-4.85
	303.15	-4.34	-4.53	-4.76
	308.15	-4.29	-4.46	-4.67
	313.15	-4.22	-4.39	-4.58
	318.15	-4.16	-4.30	-4.48
[C_3C_1pip][PF_6]	288.15	-4.72	-4.97	-5.69
	293.15	-4.67	-4.91	-5.57
	298.15	-4.62	-4.84	-5.45
	303.15	-4.57	-4.76	-5.32
	308.15	-4.50	-4.68	-5.19
	313.15	-4.44	-4.60	-5.05
	318.15	-4.37	-4.51	-4.92
[N_{4444}][PF_6]	288.15	-11.0	-11.4	-11.8
	293.15	-10.9	-11.3	-11.7
	298.15	-10.8	-11.2	-11.5
	303.15	-10.7	-11.0	-11.4
	308.15	-10.6	-10.9	-11.2

	313.15	-10.4	-10.7	-11.1
	318.15	-10.3	-10.6	-10.9
$[P_{4444}][PF_6]$	288.15	-10.6	-10.6	-10.9
	293.15	-10.5	-10.5	-10.8
	298.15	-10.4	-10.4	-10.7
	303.15	-10.3	-10.3	-10.6
	308.15	-10.2	-10.2	-10.5
	313.15	-10.1	-10.1	-10.3
	318.15	-9.9	-9.9	-10.2

3.7. Impact of the cation symmetry on the mutual solubilities between Water and imidazolium-based ionic liquids

Mónia A. R. Martins, Catarina M. S. S. Neves, Kiki A. Kurnia, Andreia Luís, Luís M. N. B. F. Santos, Mara G. Freire, Simão P. Pinho and João A. P. Coutinho, Fluid Phase Equilibria 375 (2014) 161-167, DOI: 10.1016/j.fluid.2014.05.013

MUTUAL SOLUBILITIES MEASUREMENTS

Table S 3.10. Experimental mole fraction solubility of water (x_w) in ILs, and respective standard deviations, as a function of temperature and at 0.10 MPa.

T/K	$[C_1C_1im][NTf_2]$	$[C_2C_2im][NTf_2]$	$[C_3C_3im][NTf_2]$	$[C_4C_4im][NTf_2]$	$[C_5C_5im][NTf_2]$
			x_w		
288.15	0.312 ± 0.002	0.241 ± 0.004	0.194 ± 0.007	0.159 ± 0.004	0.132 ± 0.002
293.15	0.335 ± 0.002	0.261 ± 0.001	0.206 ± 0.001	0.172 ± 0.001	0.148 ± 0.001
298.15	0.354 ± 0.004	0.277 ± 0.001	0.223 ± 0.001	0.184 ± 0.003	0.158 ± 0.001
303.15	0.376 ± 0.001	0.290 ± 0.001	0.240 ± 0.002	0.196 ± 0.002	0.170 ± 0.001
308.15	0.395 ± 0.001	0.305 ± 0.002	0.255 ± 0.002	0.207 ± 0.002	0.184 ± 0.002
313.15	0.424 ± 0.006	0.322 ± 0.002	0.270 ± 0.001	0.219 ± 0.006	0.197 ± 0.001
318.15	0.451 ± 0.007	0.341 ± 0.001	0.285 ± 0.003	0.233 ± 0.002	0.209 ± 0.002

Table S 3.11. Experimental mole fraction solubility of ionic liquid (x_{IL}) in water, and respective standard deviations, as a function of temperature and at 0.10 MPa.

T/K	$[C_1C_1im][NTf_2]$	$[C_2C_2im][NTf_2]$	$[C_3C_3im][NTf_2]$	$[C_4C_4im][NTf_2]$	$[C_5C_5im][NTf_2]$
	$10^3 \cdot x_{IL}$	$10^4 \cdot x_{IL}$	$10^4 \cdot x_{IL}$	$10^5 \cdot x_{IL}$	$10^5 \cdot x_{IL}$
288.15	1.38 ± 0.03	5.23 ± 0.04	1.82 ± 0.02	6.89 ± 0.02	1.94 ± 0.03
293.15	1.42 ± 0.01	5.31 ± 0.03	1.86 ± 0.01	7.03 ± 0.02	2.05 ± 0.08
298.15	1.49 ± 0.01	5.36 ± 0.01	1.92 ± 0.02	7.25 ± 0.01	2.11 ± 0.02

303.15	1.60 ± 0.02	5.79 ± 0.04	2.00 ± 0.01	7.62 ± 0.01	2.23 ± 0.01
308.15	1.69 ± 0.01	6.13 ± 0.05	2.06 ± 0.04	7.90 ± 0.07	2.35 ± 0.01
313.15	1.72 ± 0.01	6.50 ± 0.06	2.14 ± 0.02	9.00 ± 0.06	2.50 ± 0.02
318.15	2.03 ± 0.02	7.04 ± 0.08	2.25 ± 0.02	9.61 ± 0.07	2.71 ± 0.04

COSMO-RS

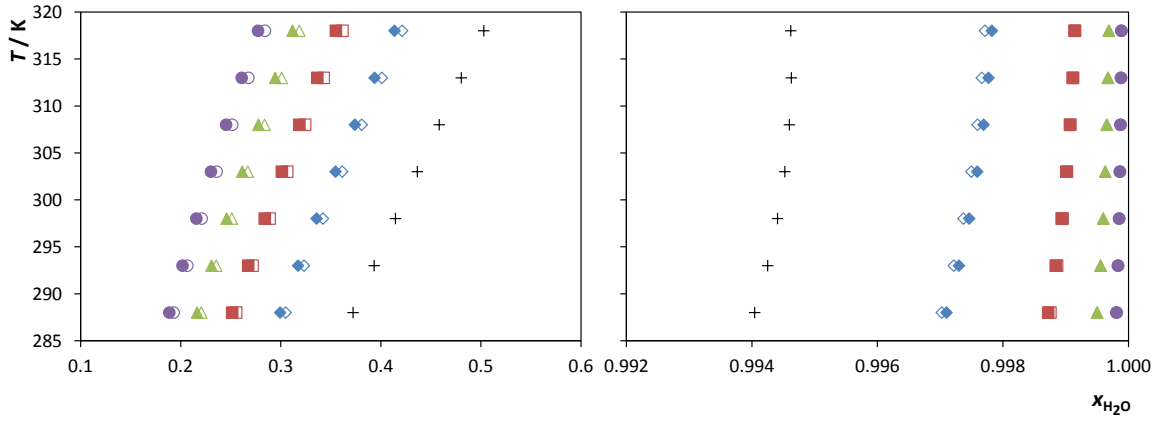

Figure S 3.14. Liquid-liquid phase diagram for water and ILs with the same number of alkyl side chain, *N*, estimate by COSMO-RS using file parameterization, BP_TZVP_C30_1301. Symbols: (+), $[C_1C_1im][NTf_2]$; (◆),$[C_2C_2im][NTf_2]$; (◇),$[C_3C_1im][NTf_2]$;(■), $[C_3C_3im][NTf_2]$; (□),$[C_5C_1im][NTf_2]$; (▲), $[C_4C_4im][NTf_2]$; (△), $[C_7C_1im][NTf_2]$; (●), $[C_5C_5im][NTf_2]$; and (○), $[C_9C_1im][NTf_2]$.

3.8. Analysis of the isomerism effect on the mutual solubilities of bis(trifluoromethylsulfonyl)imide-based ionic liquids with water

Mónia A. R. Martins, Catarina M. S. S. Neves, Kiki A. Kurnia, Luís M. N. B. F. Santos, Mara G. Freire, Simão P. Pinho, and João A. P. Coutinho, Fluid Phase Equilibria 381 (2014) 28-35, DOI: 10.1016/j.fluid.2014.08.007

MUTUAL SOLUBILITIES MEASUREMENTS

Table S 3.12. Experimental mole fraction solubility of water in ILs, x_w, and ionic iquid in water, x_{IL}, at different temperatures and at 0.10 MPa, and respective standard deviations.

T/K	$[C_1im][NTf_2]$	$[C_2im][NTf_2]$	$[C_2C_3im][NTf_2]$	$[C_4C_1C_1im][NTf_2]$
		x_w		
288.15	0.627 ± 0.009	0.604 ± 0.010	0.209 ± 0.002	0.168 ± 0.001
293.15	0.648 ± 0.003	0.612 ± 0.010	0.222 ± 0.002	0.183 ± 0.002
298.15	0.667 ± 0.005	0.628 ± 0.006	0.239 ± 0.001	0.191 ± 0.001

303.15	0.686 ± 0.001	0.641 ± 0.004	0.256 ± 0.001	0.212 ± 0.001
308.15	0.709 ± 0.001	0.659 ± 0.005	0.278 ± 0.006	0.229 ± 0.001
313.15	0.720 ± 0.003	0.673 ± 0.007	0.296 ± 0.003	0.244 ± 0.002
318.15	0.736 ± 0.010	0.682 ± 0.012	0.314 ± 0.003	0.263 ± 0.001
T/K			$10^3 x_{IL}$	
288.15	4.132 ± 0.037	2.360 ± 0.004	0.311 ± 0.001	0.203 ± 0.002
293.15	4.206 ± 0.027	2.388 ± 0.019	0.317 ± 0.001	0.206 ± 0.008
298.15	4.359 ± 0.011	2.451 ± 0.008	0.325 ± 0.001	0.209 ± 0.001
303.15	4.499 ± 0.053	2.549 ± 0.001	0.336 ± 0.002	0.217 ± 0.003
308.15	4.811 ± 0.032	2.669 ± 0.019	0.351 ± 0.002	0.237 ± 0.001
313.15	5.393 ± 0.020	2.979 ± 0.060	0.387 ± 0.002	0.246 ± 0.003
318.15	5.945 ± 0.026	3.233 ± 0.010	0.410 ± 0.014	0.270 ± 0.001

THERMODYNAMIC FUNCTIONS OF SOLUTION

Table S 3.13. Correlation parameters for the mole fraction solubility of water in the IL-rich phase and IL in the water-rich phase using eqs 3.1 and 3.2, and respective standard deviations.

IL	*A*	*B* / K	*C*	*D* / K	*E*
[C_1im][NTf_2]	1.252 ± 0.055	-494.1 ± 16.6	-554.0 ± 62.7	23802.9 ± 2826.8	82.3 ± 9.3
[C_2im][NTf_2]	0.853 ± 0.051	-392.4 ± 15.5	-503.6 ± 60.9	21623.2 ± 2746.8	74.6 ± 9.1
[C_2C_3im][NTf_2]	2.860 ± 0.084	-1277.7 ± 25.3	-382.0 ± 61.3	16139.1 ± 2764.5	56.1 ± 9.1
[$C_4C_1C_1$im][NTf_2]	2.987 ± 0.145	-1376.3 ± 43.9	-390.6 ± 68.7	16495.2 ± 3098.6	57.4 ± 10.2

COSMO-RS

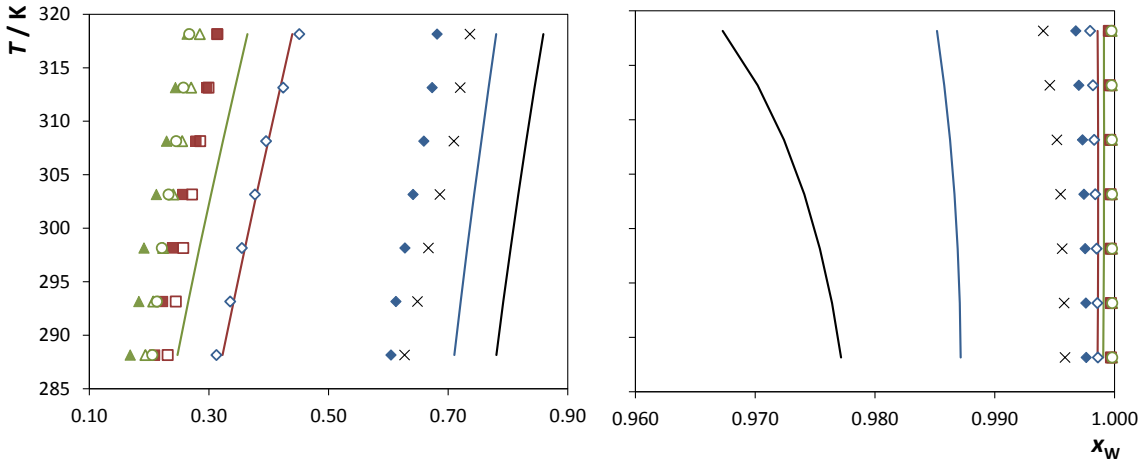

Figure S 3.15. Liquid-liquid phase diagram for water and ILs: (×), [C_1im][NTf_2]; (◆), [C_2im][NTf_2]; (◇), [C_1C_1im][NTf_2]; (■), [C_2C_3im][NTf_2]; (□), [C_4C_1im][NTf_2]; (▲), [$C_4C_1C_1$im][NTf_2]; (△), [C_3C_3im][NTf_2]; and (○), [C_5C_1im][NTf_2]. The lines at the same colours represent the COSMO-RS predictions using the file parameterization BP_TZVP_C30_1401.

3.9. The impact of ionic liquids fluorinated moieties on their thermophysical properties and aqueous phase behaviour

Catarina M. S. S. Neves, Kiki Adi Kurnia, Karina Shimizu, Isabel M. Marrucho, Luís Paulo N. Rebelo, João A. P. Coutinho, Mara G. Freire, José N. Canongia Lopes, Physical Chemistry Chemical Physics 16 (2014) 21340-21348, DOI: 10.1039/C4CP02008A

NMR SPECTRUM

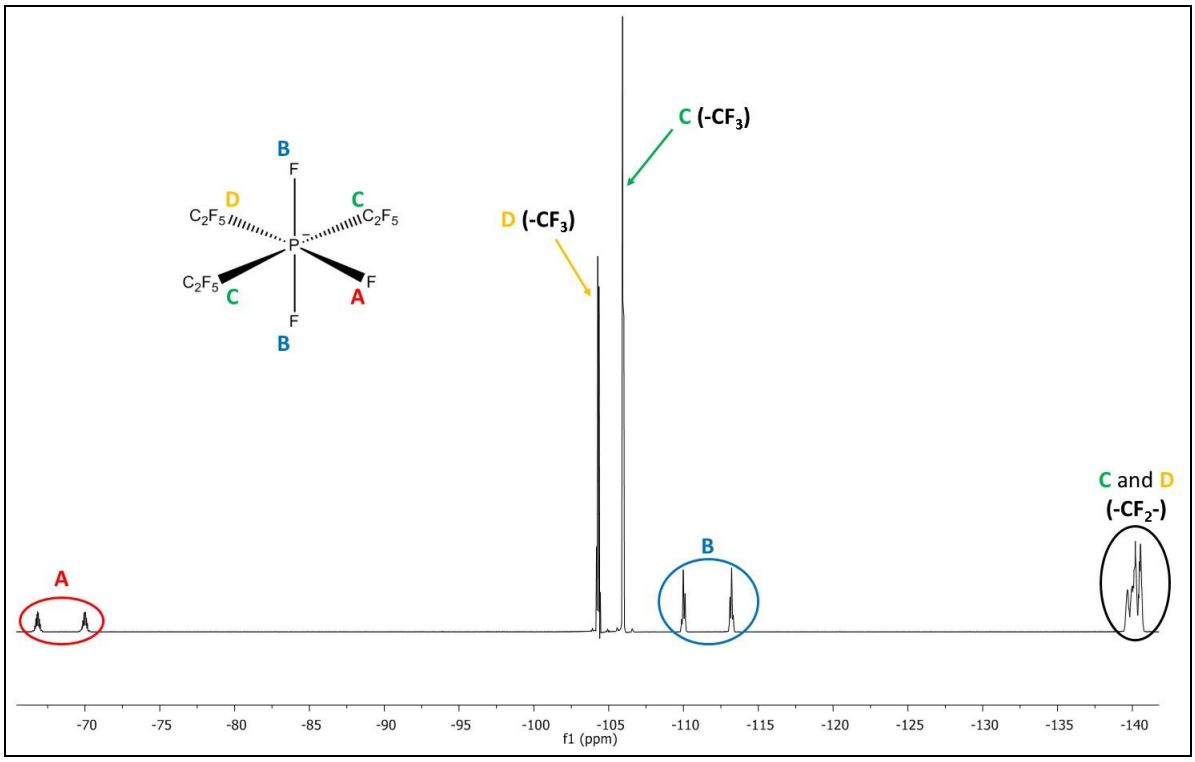

Figure S 3.16. ^{19}F NMR spectra of $[C_2C_1im][FAP]$.

DENSITY AND VISCOSITY

Table S 3.14. Experimental density, ρ, and viscosity, η, for pure ILs as function of temperature and at 0.1 MPa.

T / K	ρ / (kg·m^{-3})		η / (mPa·s)	
	$[C_2C_1im][FAP]$	$[C_2C_1im][PF_6]$	$[C_2C_1im][FAP]$	$[C_2C_1im][PF_6]$
278.15	1726.7	---	168.750	---
283.15	1720.6	---	126.710	---
288.15	1714.5	---	97.357	---

293.15	1708.1	---	76.410	---
298.15	1701.6	---	61.022	---
303.15	1695.0	---	49.617	---
308.15	1688.3	---	40.934	---
313.15	1681.6	---	34.213	---
318.15	1674.9	---	28.934	---
323.15	1668.2	---	24.722	---
328.15	1661.5	---	21.327	---
333.15	1654.8	---	18.552	---
338.15	1648.4	1437.6	16.263	26.830
343.15	1641.9	1433.3	14.355	23.296
348.15	1635.4	1429.1	12.726	20.330
353.15	1629.1	1424.8	11.371	17.920
358.15	1622.8	1420.6	10.216	15.810
363.15	1616.6	1416.4	9.223	14.075

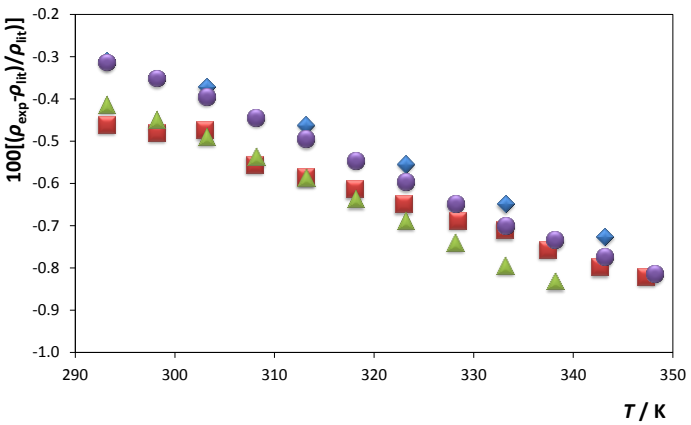

Figure S 3.17. Relative deviations between the experimental densities measured in this work (ρ_{exp}) and those reported in literature (ρ_{lit}) as a function of temperature for [C_2C_1im][FAP]: ●, Seki et al.[9]; ▲, Liu et al.[10]; ◆, Almantariotis et al.[11]; ■, Součková et al.[12].

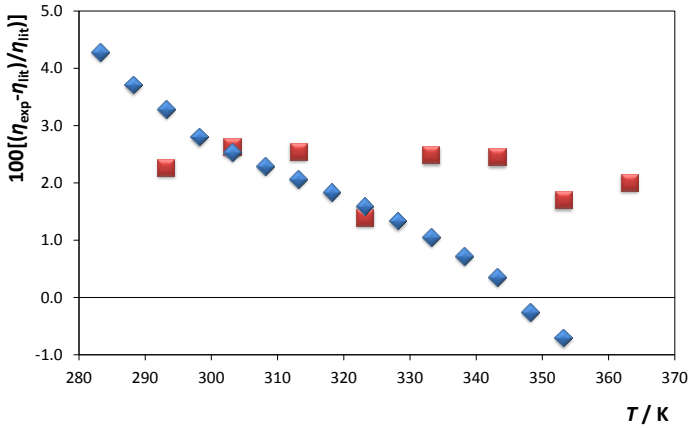

Figure S 3.18. Relative deviations between the experimental viscosities measured in this work (η_{exp}) and those reported in literature (η_{lit}) as a function of temperature for [C_2C_1im][FAP]: ◆, Seki et al.[9]; ■, Almantariotis et al.[11].

MUTUAL SOLUBILITIES MEASUREMENTS

Table S 3.15. Experimental mole fraction solubility of water in ILs, x_w, and of ILs in water, x_{IL}, as a function of temperature and at 0.1 MPa.

	[C_2C_1im][FAP]		[C_2C_1im][PF_6]	
T / K	$10^5 \times (x_{IL} \pm \sigma^a)$	$10^1 \times (x_w \pm \sigma^a)$	$10^2 \times (x_{IL} \pm \sigma^a)$	$x_w \pm \sigma^a$
288.15	0.999 ± 0.014	0.577 ± 0.008	0.167 ± 0.003	---
293.15	1.325 ± 0.034	0.614 ± 0.021	0.260 ± 0.008	---
298.15	1.624 ± 0.024	0.682 ± 0.011	0.288 ± 0.002	---
303.15	1.805 ± 0.019	0.769 ± 0.006	0.567 ± 0.005	---
308.15	1.965 ± 0.238	0.835 ± 0.018	0.848 ± 0.006	---
313.15	2.164 ± 0.041	0.923 ± 0.022	1.027 ± 0.003	---
318.15	2.483 ± 0.009	1.010 ± 0.018	1.148 ± 0.004	---
333.15	3.011 ± 0.066	1.387 ± 0.001	1.785 ± 0.082	---
338.15	3.313 ± 0.007	1.541 ± 0.012	1.973 ± 0.072	---
343.15	3.643 ± 0.036	1.633 ± 0.070	2.191 ± 0.078	0.644 ± 0.015
348.15	3.845 ± 0.004	1.756 ± 0.018	2.365 ± 0.086	0.694 ± 0.024
353.15	4.070 ± 0.010	1.831 ± 0.006	2.529 ± 0.083	0.733 ± 0.011
358.15	4.499 ± 0.021	1.947 ± 0.007	2.712 ± 0.079	0.765 ± 0.004
363.15	4.753 ± 0.058	2.073 ± 0.024	2.934 ± 0.073	0.802 ± 0.074

[a] Standard deviation

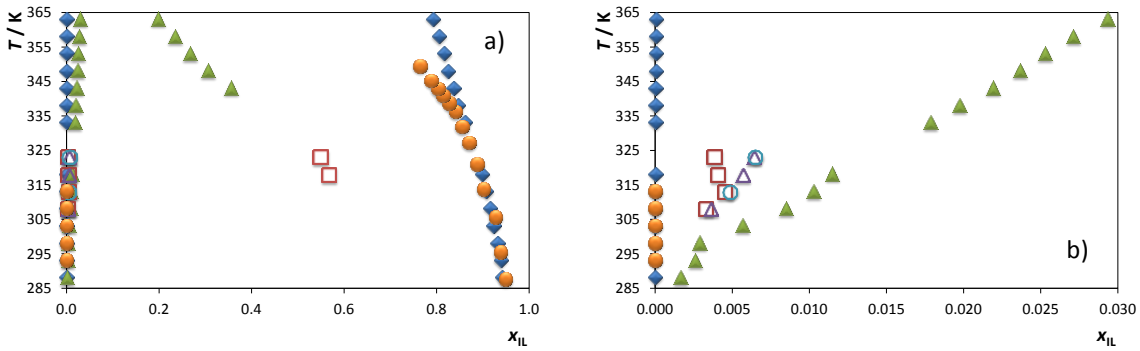

Figure S 3.19. LLE phase diagrams obtained in this work (▲, $[C_2C_1im][PF_6]$; ◆, $[C_2C_1im][FAP]$) and those reported in literature: □, Wong et al.[13] with values obtained by KF; ○, Wong et al.[13] with values obtained by UV; △, Wong et al.[13] with values obtained by TGA; ●, Domańska et al.[14] with values obtained by UV (solubility of IL in water) and dynamic (synthetic) method (solubility of water in IL).

MOLECULAR DYNAMICS SIMULATION

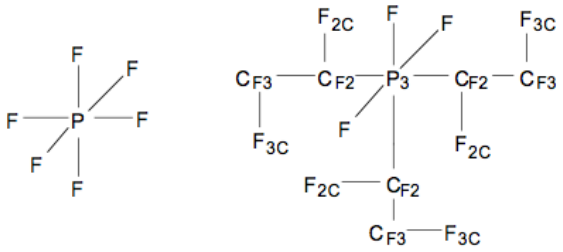

Figure S 3.20. Nomenclature adopted for the atomistic force-field modeling of the $[PF_6]^-$ (left) and $[FAP]^-$ (right) anions (equivalent atoms are not shown in the latter scheme for clarity reasons).

Table S 3.16. Force field non-bonded parameters – atomic point charges (q), Lennard-Jones diameter and interaction parameters (σ_{LJ} and ε_{LJ}) – for the $[PF_6]^-$ and $[FAP]^-$ anions adopted in this work.[15–18] The different partial charges conferred to each type of atom in the two ions are highlighted in bold. These were calculated using quantum-mechanics methods described in literature.[16–18]

$[PF_6]^-$ [15–17]			
Atom	q (a.c.u.)	σ_{LJ} (10^{-10}m)	ε_{LJ} / (kJ·mol^{-1})
P	**1.34**	3.74	0.8368
F	**-0.39**	3.12	0.2552
$[FAP]^-$ [18]			
P3	**0.62**	3.74	0.8368
CF2	**0.24**	3.50	0.27614
F2C	**-0.12**	3.12	0.25520
CF3	**0.42**	3.50	0.27614
F3C	-0.19	3.12	0.2552

Appendix Chapter 4 – Removing Ionic Liquids from Aqueous Solutions Using Aqueous Biphasic Systems

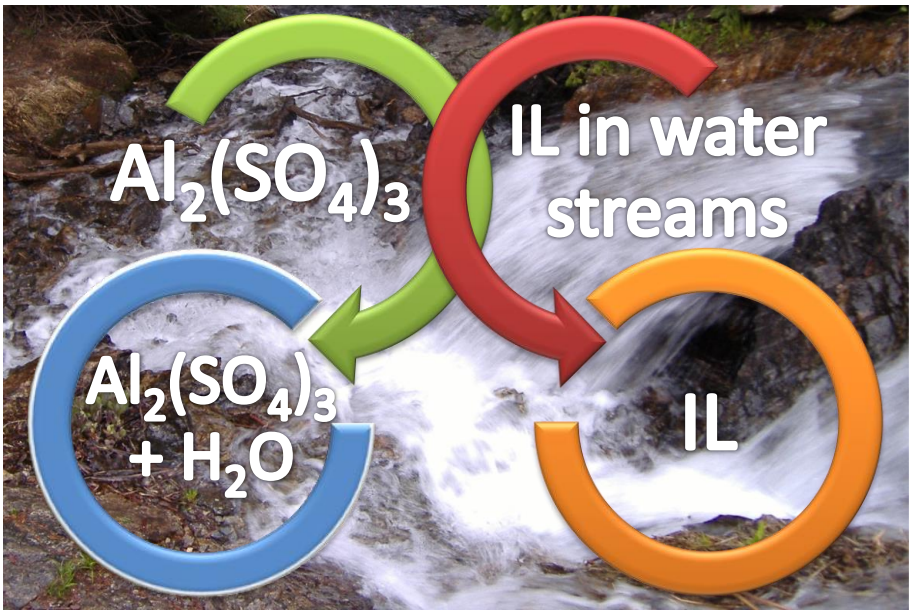

4.3. Improved recovery of ionic liquids from contaminated aqueous streams using aluminium-based salts

Catarina M. S. S. Neves, Mara G. Freire and João A. P. Coutinho, RSC Advances 2 (2012) 10882-10890, DOI: 10.1039/C2RA21535G

The experimental solubility data obtained, at 298 K and at atmospheric pressure, are presented in Tables S4.1 and S4.2. Figure S4.1 depicts the gathered results in molality units. It should be remarked that for the salt $AlK(SO_4)_2$ the concentrations reported were calculated without the contribution of the water complexed with the salt.

Table S 4.1. Experimental mass fraction data for the system composed of IL (1) + $Al_2(SO_4)_3$ (2) + H_2O (3) at 298 K.

$[C_2C_1im][CF_3SO_3]$ M_w = 260.23					
100 w_1	100 w_2	100 w_1	100 w_2	100 w_1	100 w_2
12.997	27.292	27.011	15.625	34.456	10.650
13.985	26.307	27.543	15.183	34.757	10.415
14.961	25.337	28.056	14.869	35.173	10.164
15.741	24.571	28.564	14.493	35.537	9.964
16.570	23.764	29.051	14.143	35.855	9.766
17.707	22.861	29.646	13.790	35.988	9.522
18.762	22.000	30.060	13.454	36.289	9.389
19.830	21.129	30.415	13.178	36.580	9.177
20.783	20.361	30.874	12.882	37.464	8.948
21.386	19.901	31.349	12.567	37.720	8.752
22.278	19.228	31.746	12.305	38.376	8.495
23.044	18.613	32.111	12.039	38.663	8.239
23.697	18.057	32.633	11.745	39.826	7.911
24.117	17.617	32.802	11.538	40.385	7.202
25.149	16.972	32.980	11.377	42.004	6.656
25.849	16.512	33.377	11.152	44.480	6.048
26.462	16.055	33.975	10.857		
$[C_4C_1im][CF_3SO_3]$ M_w = 288.28					
100 w_1	100 w_2	100 w_1	100 w_2	100 w_1	100 w_2
4.151	27.119	17.233	11.710	26.368	7.931
5.162	25.205	17.598	11.538	27.239	7.678
6.264	23.134	18.224	11.106	28.220	7.347

6.767	22.060	18.530	10.868	29.226	7.045
8.727	19.385	18.945	10.753	30.307	6.729
9.873	17.908	19.466	10.530	31.766	6.400
10.666	16.970	19.985	10.316	33.136	5.992
11.398	16.264	20.469	10.152	34.565	5.555
12.069	15.550	20.865	9.857	36.370	5.178
12.599	15.053	21.567	9.700	38.470	4.742
14.160	13.784	22.186	9.398	40.565	4.122
14.676	13.333	22.889	9.191	44.066	3.620
15.177	13.131	23.355	8.827	48.718	2.819
15.872	12.621	24.076	8.621	51.022	2.065
16.346	12.230	24.809	8.430	57.809	1.074
16.672	12.114	25.555	8.194		

$[C_4C_1im][Tos]$ M_w = 310.42

100 w_1	100 w_2	100 w_1	100 w_2	100 w_1	100 w_2
7.659	27.371	16.398	20.827	35.211	10.339
8.613	26.487	17.750	19.966	37.797	9.288
9.448	25.775	18.819	19.343	39.529	8.942
10.347	25.038	20.745	18.143	42.944	7.621
11.217	24.364	22.789	16.923	45.492	6.956
12.192	23.633	24.732	15.859	48.439	6.224
13.127	22.995	27.420	14.272	51.902	5.310
14.167	22.275	29.885	12.959		
15.204	21.608	32.373	11.735		

$[C_4C_1im][N(CN)_2]$ M_w = 205.26

100 w_1	100 w_2	100 w_1	100 w_2	100 w_1	100 w_2
8.893	26.678	21.133	16.414	35.688	7.255
11.229	24.349	22.458	15.449	37.576	6.234
12.870	22.789	23.644	14.584	39.024	5.807
13.926	21.837	24.318	14.159	40.387	5.179
15.222	20.784	25.877	13.069	41.762	4.611
16.141	20.063	27.194	12.199	43.816	3.989
16.842	19.531	28.687	11.195	45.372	3.289
17.502	19.034	29.765	10.577	47.133	2.543
18.244	18.487	31.021	9.862	49.885	1.851
19.318	17.686	33.106	8.621	58.498	0.800
20.140	17.111	34.005	8.216		

$[C_8py][N(CN)_2]$ M_w = 258.36

100 w_1	100 w_2	100 w_1	100 w_2	100 w_1	100 w_2

1.430	35.132	12.491	12.294	20.066	8.014
2.116	30.754	12.777	12.150	20.542	7.801
2.608	28.773	13.124	11.995	21.190	7.636
3.071	26.845	13.413	11.741	21.704	7.433
3.469	25.118	13.717	11.482	22.204	7.222
3.929	24.058	14.028	11.217	22.821	7.000
4.712	22.543	14.227	11.117	23.577	6.744
5.510	20.994	14.387	10.974	24.323	6.483
5.811	19.245	14.550	10.839	25.007	6.200
7.167	17.499	14.799	10.745	25.953	5.949
8.021	16.258	14.965	10.609	26.741	5.603
8.579	15.619	15.159	10.470	27.991	5.351
9.137	15.072	15.411	10.361	29.329	5.040
9.515	14.714	15.605	10.218	30.624	4.655
9.816	14.397	15.876	10.106	32.098	4.245
10.147	14.091	16.239	10.035	34.384	3.886
10.416	13.852	16.714	9.761	37.033	3.423
10.736	13.661	17.180	9.402	40.237	2.934
11.032	13.392	17.506	9.243	45.576	2.385
11.326	13.134	17.848	9.089	49.903	1.855
11.578	12.985	18.313	8.992	59.041	1.000
11.828	12.844	19.028	8.655		
12.072	12.646	19.635	8.210		
$[(C_7H_7)C_1im][C_2H_5SO_4]$ M_w = 298.36					
100 w_1	100 w_2	100 w_1	100 w_2	100 w_1	100 w_2
10.211	31.136	30.872	14.733	30.872	14.733
12.491	29.191	31.694	14.183	31.694	14.183
13.403	27.885	32.268	13.743	32.268	13.743
15.218	26.299	33.052	13.228	33.052	13.228
17.315	24.811	33.922	12.730	33.922	12.730
18.807	23.490	34.556	12.303	34.556	12.303
20.350	22.323	35.371	11.865	35.371	11.865
21.674	21.304	35.676	11.568	35.676	11.568
22.614	20.381	36.504	11.167	36.504	11.167
24.219	19.344	37.062	10.844	37.062	10.844
25.128	18.620	37.561	10.542	37.561	10.542
26.252	17.853	38.080	10.229	38.080	10.229
27.457	17.115	38.619	9.942	38.619	9.942
28.487	16.412	39.209	9.672	39.209	9.672

29.221	15.849	39.791	9.376	39.791	9.376
29.763	15.348	40.360	9.096		

$[P_{i(444)1}][Tos]$ M_w = 385.52

100 w_1	100 w_2	100 w_1	100 w_2	100 w_1	100 w_2
6.968	19.962	11.100	16.959	18.869	13.064
7.075	19.880	11.342	16.754	19.319	12.935
7.188	19.790	11.501	16.713	19.807	12.776
7.351	19.618	11.749	16.545	20.590	12.261
7.533	19.424	11.913	16.520	21.113	12.097
7.667	19.328	12.204	16.305	21.651	11.925
7.810	19.225	12.397	16.245	22.581	11.360
8.013	18.999	12.705	16.032	23.227	11.122
8.164	18.892	12.906	15.970	23.926	10.854
8.321	18.769	13.238	15.748	24.584	10.614
8.487	18.650	13.460	15.697	25.307	10.322
8.650	18.491	13.827	15.436	26.060	10.045
8.838	18.344	14.061	15.362	27.360	9.312
9.028	18.177	14.316	15.282	28.252	9.040
9.199	18.055	14.559	15.201	29.179	8.705
9.381	17.917	14.954	14.942	30.242	8.352
9.500	17.890	15.212	14.853	32.040	8.047
9.690	17.737	15.487	14.749	33.353	7.583
9.895	17.577	15.915	14.457	34.777	7.094
10.029	17.547	16.207	14.356	36.186	6.634
10.234	17.391	16.512	14.264	38.604	6.231
10.358	17.356	16.820	14.164	41.588	5.788
10.571	17.200	17.382	13.795	44.969	5.303
10.718	17.187	17.762	13.674	49.247	4.675
10.959	17.003	18.160	13.538	54.358	3.894

$[P_{4444}]Br$ M_w = 339.34

100 w_1	100 w_2	100 w_1	100 w_2	100 w_1	100 w_2
4.190	21.128	9.087	15.820	15.425	11.634
4.379	20.908	9.273	15.633	15.948	11.205
4.552	20.640	9.394	15.578	16.318	11.019
4.721	20.419	9.596	15.367	16.692	10.857
4.888	20.147	9.726	15.314	17.105	10.679
5.013	20.010	9.938	15.097	17.990	10.235
5.136	19.862	10.078	15.032	18.723	9.663
5.274	19.694	10.295	14.812	19.803	9.111

5.453	19.465	10.444	14.759	20.319	8.885
5.611	19.288	10.600	14.696	20.930	8.628
5.776	19.099	11.300	14.113	23.349	7.690
5.950	18.921	11.475	14.021	24.120	7.339
6.113	18.747	11.639	13.965	24.936	6.956
6.293	18.547	11.929	13.695	25.743	6.636
6.540	18.184	12.128	13.604	27.239	6.299
6.752	17.955	12.467	13.293	28.329	5.788
6.977	17.745	12.704	13.197	29.943	5.443
7.203	17.508	12.912	13.101	32.009	4.952
7.408	17.351	13.261	12.778	34.363	4.431
7.675	17.053	13.486	12.674	37.818	3.917
7.810	16.919	13.740	12.565	46.099	3.370
8.042	16.733	14.148	12.232	52.891	2.920
8.299	16.527	14.432	12.107	23.349	7.690
8.457	16.372	14.740	11.973	24.120	7.339
8.732	16.160	11.300	14.113		
8.904	15.985	11.475	14.021		

$[P_{4444}]Cl$ M_w = 294.89

100 w_1	100 w_2	100 w_1	100 w_2	100 w_1	100 w_2
4.829	26.091	9.462	20.463	19.113	12.385
5.033	25.786	9.818	20.089	19.805	11.959
5.226	25.503	10.198	19.700	20.535	11.573
5.410	25.246	10.530	19.388	21.320	11.168
5.586	25.016	10.948	18.983	22.028	10.757
5.786	24.743	11.321	18.653	22.866	10.252
6.079	24.308	11.742	18.254	23.793	9.696
6.292	24.042	12.165	17.882	24.460	9.478
6.549	23.709	12.655	17.451	25.142	9.200
6.789	23.416	13.047	17.132	26.653	8.642
7.011	23.151	13.491	16.786	27.850	7.969
7.283	22.823	14.040	16.291	28.731	7.707
7.539	22.526	14.650	15.730	29.809	7.406
7.815	22.213	15.186	15.296	30.945	7.036
8.063	21.954	15.741	14.874	32.596	6.803
8.303	21.695	16.364	14.382	33.846	6.398
8.574	21.403	17.015	13.883	36.683	6.171
8.894	21.028	17.528	13.587	39.580	5.731
9.190	20.719	18.289	13.006	41.527	5.178

$[P_{4441}][CH_3SO_4]$ M_w = 358.52					
100 w_1	100 w_2	100 w_1	100 w_2	100 w_1	100 w_2
7.253	22.156	16.210	14.507	26.822	8.406
8.475	20.764	17.251	13.872	28.281	7.543
9.010	20.136	19.481	12.616	29.473	7.005
10.616	18.751	20.295	12.054	30.426	6.748
11.226	18.252	21.115	11.548	31.807	6.168
11.904	17.641	22.125	10.820	33.864	5.682
12.643	17.074	22.834	10.526	36.390	4.975
13.240	16.723	23.926	9.819	39.395	4.193
14.166	15.977	24.590	9.574	50.781	3.265
15.269	15.097	25.836	8.819	56.178	2.762

Table S 4.2. Experimental mass fraction data for the system composed of IL (1) + $AlK(SO_4)_2$ (2) + H_2O (3) at 298 K.

$[C_4C_1im][CF_3SO_3]$ M_w = 288.28					
100 w_1	100 w_2	100 w_1	100 w_2	100 w_1	100 w_2
28.905	4.312	37.099	3.018	42.396	2.287
29.415	4.219	37.411	2.964	42.723	2.247
29.673	4.121	37.923	2.903	42.959	2.212
29.892	4.088	38.256	2.850	43.333	2.170
30.915	3.954	38.553	2.807	43.651	2.133
31.427	3.857	39.024	2.743	43.815	2.115
32.003	3.759	39.327	2.698	44.303	2.053
32.568	3.669	39.574	2.671	44.534	2.024
33.145	3.585	39.872	2.625	45.107	1.961
33.694	3.502	40.335	2.553	45.618	1.902
34.260	3.412	40.856	2.499	46.095	1.851
34.823	3.331	41.097	2.458	46.450	1.821
35.737	3.203	41.441	2.409	54.621	1.010
35.991	3.163	41.812	2.365	61.240	0.612
36.696	3.073	42.046	2.329	65.196	0.424
$[C_8py][N(CN)_2]$ M_w = 258.36					
100 w_1	100 w_2	100 w_1	100 w_2	100 w_1	100 w_2
22.417	4.613	30.612	3.349	35.460	2.649
22.861	4.513	31.045	3.282	36.387	2.291
23.444	4.389	31.466	3.213	38.301	2.075
23.990	4.297	31.815	3.165	40.321	1.865
24.660	4.192	32.092	3.113	42.313	1.678

25.713	4.022	32.543	3.051	43.970	1.527
26.170	3.941	33.052	2.984	45.465	1.408
27.023	3.831	33.541	2.922	46.850	1.304
27.560	3.752	33.750	2.875	48.893	1.151
28.050	3.672	34.266	2.811	61.431	0.501
28.392	3.610	34.673	2.759	64.680	0.390
29.675	3.486	34.780	2.732	67.666	0.293
29.967	3.425	35.014	2.695		

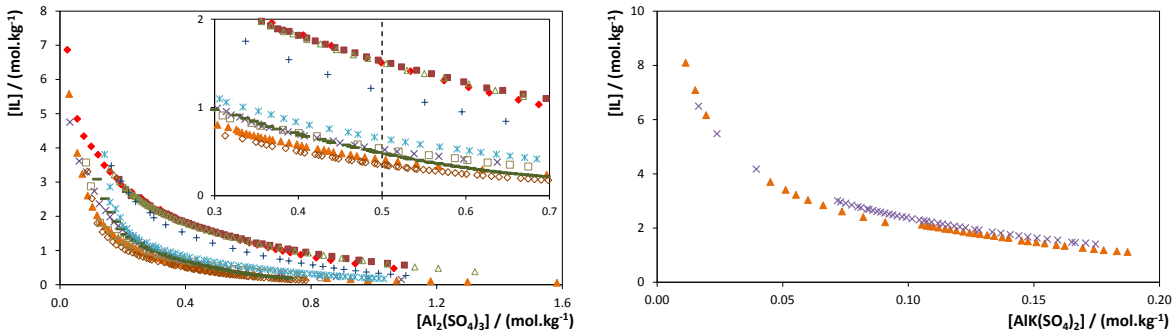

Figure S 4.1. Ternary phase diagrams for the systems composed of IL + aluminium-based salt + water at 298 K and atmospheric pressure (molality units): ■, $[C_2C_1im][CF_3SO_3]$; ×, $[C_4C_1im][CF_3SO_3]$; ●, $[C_4C_1im][SCN]$; +, $[C_4C_1im][Tos]$; ◆, $[C_4C_1im][N(CN)_2]$;▲, $[C_8py][N(CN)_2]$; △, $[(C_7H_7)C_1im][C_2H_5SO_4]$; ▬, $[P_{i(444)1}][Tos]$; ◇, $[P_{4444}]Br$; ✳, $[P_{4444}]Cl$; □, $[P_{4441}][CH_3SO_4]$.

Table S 4.3. Critical point of each system composed of IL + $Al_2(SO_4)_3$ + H_2O at 298 K and respective values obtained from the fitting.

IL	*f*	*g*	R^2	Critical Point / wt%	
				[*IL*]	[*Salt*]
$[C_2C_1im][CF_3SO_3]$	1.327	9.722	0.9926	14.32	28.72
$[C_4C_1im][CF_3SO_3]$	0.716	56.085	0.8568	1.49	57.15
$[C_4C_1im][Tos]$	1.268	-1.893	0.9895	17.88	20.79
$[C_4C_1im][N(CN)_2]$	2.034	-23.422	0.9292	19.72	16.68
$[C_8py][N(CN)_2]$	1.044	35.283	0.9747	3.13	38.55
$[(C_7H_7)C_1im][C_2H_5SO_4]$	1.273	5.979	0.9970	16.91	27.50
$[P_{i(444)1}][Tos]$	1.924	-13.816	0.9816	14.86	14.78
$[P_{4444}]Br$	1.846	8.992	0.9997	7.72	23.25
$[P_{4444}]Cl$	0.656	30.910	0.8203	35.03	6.29
$[P_{4441}][CH_3SO_4]$	1.714	-1.610	0.9193	12.05	19.04

Table S 4.4. Experimental density (ρ) and viscosity (η) data of the coexisting phases in diverse ABS composed of 40 wt% of IL + 15 wt% of $Al_2(SO_4)_3$ + 45 wt% of H_2O in the temperature range between 298.15 K and 328.15 K.

IL	Phase	*T*	*P*	*H*
		K	g·cm^{-3}	mPa·s
			$Al_2(SO_4)_3$	
$[C_4C_1im][CF_3SO_3]$	IL – rich phase	298.15	1.2374	3.7387
		308.15	1.2296	2.8957
		318.15	1.2215	2.3083
		328.15	1.2132	1.8999
	Salt – rich phase	298.15	1.2899	12.128
		308.15	1.2842	8.5076
		318.15	1.2780	6.1348
		328.15	1.2710	4.5322
$[C_8py][N(CN)_2]$	IL – rich phase	298.15	1.0105	11.372
		308.15	1.0040	8.1779
		318.15	0.9935	5.9367
		328.15	0.9812	4.5779
	Salt – rich phase	298.15	1.2630	8.8931
		308.15	1.2576	6.4328
		318.15	1.2517	4.7492
		328.15	1.2450	3.5907
$[(C_7H_7)C_1im][EtSO_4]$	IL – rich phase	298.15	1.1642	6.9866
		308.15	1.1573	5.0923
		318.15	1.1502	3.8604
		328.15	1.1430	3.0241
	Salt – rich phase	298.15	1.3061	15.242
		308.15	1.3006	10.478
		318.15	1.2944	7.4514
		328.15	1.2876	5.4609
$[C_4C_1im][N(CN)_2]$	IL – rich phase	298.15	1.0415	4.5958
	Salt – rich phase	298.15	1.3135	17.177
		308.15	1.3076	11.664
		318.15	1.3010	8.2411
$[C_2C_1im][CF_3SO_3]$	IL – rich phase	298.15	1.2394	3.7823
		308.15	1.2314	2.9436
		318.15	1.2233	2.361
		328.15	1.2151	1.9244
	Salt – rich phase	298.15	1.2911	12.214

		308.15	1.2855	8.5628
		318.15	1.2793	6.177
		328.15	1.2723	4.5755
$[C_4C_1im][Tos]$	IL – rich phase	298.15	1.1355	9.3852
		308.15	1.1284	6.5792
		318.15	1.1211	4.8017
		328.15	1.1137	3.6367
	Salt – rich phase	298.15	1.2969	15.568
		308.15	1.2912	10.582
		318.15	1.2848	7.4506
		328.15	1.2777	5.3999
$[P_{4444}]Br$	IL – rich phase	298.15	1.0591	19.382
		308.15	1.0515	12.462
		318.15	1.0439	8.5298
		328.15	1.0362	6.1428
	Salt – rich phase	298.15	1.2696	8.1799
		308.15	1.2643	5.9425
		318.15	1.2587	4.4584
		328.15	1.2524	3.4339
$[P_{4444}]Cl$	IL – rich phase	298.15	0.9999	12.795
		308.15	0.9929	8.4367
		318.15	0.9857	5.9034
		328.15	0.9784	4.3341
	Salt – rich phase	298.15	1.2928	13.02
		308.15	1.2876	9.1173
		318.15	1.2819	6.5977
		328.15	1.2757	4.8988
$[P_{i(444)1}][Tos]$	IL – rich phase	298.15	1.0709	14.363
		308.15	1.0638	9.5221
		318.15	1.0566	6.6981
		328.15	1.0493	4.9375
	Salt – rich phase	298.15	1.2802	10.527
		308.15	1.2750	7.5126
		318.15	1.2692	5.5288
		328.15	1.2628	4.1661
$[P_{4441}][CH_3SO_4]$	IL – rich phase	298.15	1.0495	10.385
		308.15	1.0420	7.0628
		318.15	1.0346	5.0561
		328.15	1.0271	3.7836

Salt – rich phase	298.15	1.3045	14.579
	308.15	1.2991	10.117
	318.15	1.2933	7.2546
	328.15	1.2866	5.3356

The consistency of the tie-line compositions was ascertained by the empirical correlations given by Othmer–Tobias[2] (eq S4.1) and Bancroft[192] (eq S4.2).

$$\left(\frac{1-[IL]_{\text{IL}}}{[IL]_{\text{IL}}}\right) = k_1\left(\frac{1-[Salt]_{\text{Salt}}}{[Salt]_{\text{Salt}}}\right)^{n} \quad \text{(S4.1)}$$

$$\left(\frac{[H_2O]_{\text{Salt}}}{[Salt]_{\text{Salt}}}\right) = k_2\left(\frac{[H_2O]_{\text{IL}}}{[IL]_{\text{IL}}}\right)^{r} \quad \text{(S4.2)}$$

where "IL" and "Salt" designate the ionic liquid rich-phase and the salt rich-phase, respectively; [*IL*], [*Salt*] and [H_2O] represent, respectively, the weight fraction of ionic liquid, salt and water. The k_1, n, k_2 and r are fitting parameters. A linear dependency of the plots $\log\left(\frac{1-[IL]_{\text{IL}}}{[IL]_{\text{IL}}}\right)$ against $\log\left(\frac{1-[Salt]_{\text{Salt}}}{[Salt]_{\text{Salt}}}\right)$ and $\log\left(\frac{[H_2O]_{\text{Salt}}}{[Salt]_{\text{Salt}}}\right)$ against $\log\left(\frac{[H_2O]_{\text{IL}}}{[IL]_{\text{IL}}}\right)$ indicate an acceptable consistency of the results.

Table S 4.5. Values of the fitting parameters of eqs S4.1 and S4.2 for the systems composed of IL + $Al_2(SO_4)_3$ + H_2O at 298 K, and respective correlation coefficients (R^2).

IL	*Othmer – Tobias*, eq S4.1			*Bancroft*, eq S4.2		
	n	k_1	R^2	r	k_2	R^2
$[C_2C_1im][CF_3SO_3]$	1.3625	0.3385	0.9940	1.5451	0.3340	0.9920
$[C_4C_1im][CF_3SO_3]$	0.8348	0.1397	0.8129	0.9241	0.1305	0.8256
$[C_4C_1im][Tos]$	1.2994	0.6254	0.9911	1.2449	0.5726	0.9909
$[C_4C_1im][N(CN)_2]$	2.1597	0.3040	0.9175	0.4155	1.6808	0.9176
$[C_8py][N(CN)_2]$	0.1945	0.4004	0.9326	4.8194	89.5332	0.9298
$[(C_7H_7)C_1im][C_2H_5SO_4]$	1.2920	0.4474	0.9962	0.7072	1.8015	0.9970
$[P_{i(444)1}][Tos]$	1.9492	0.2628	0.9743	0.5051	2.0566	0.9740
$[P_{4444}]Br$	1.9628	0.1052	0.9985	2.0474	0.0969	0.9988
$[P_{4444}]Cl$	0.6422	0.5771	0.8135	0.6643	0.5414	0.8179

$[P_{4441}][CH_3SO_4]$	1.7494	0.2420	0.9020	0.4868	2.1296	0.9039

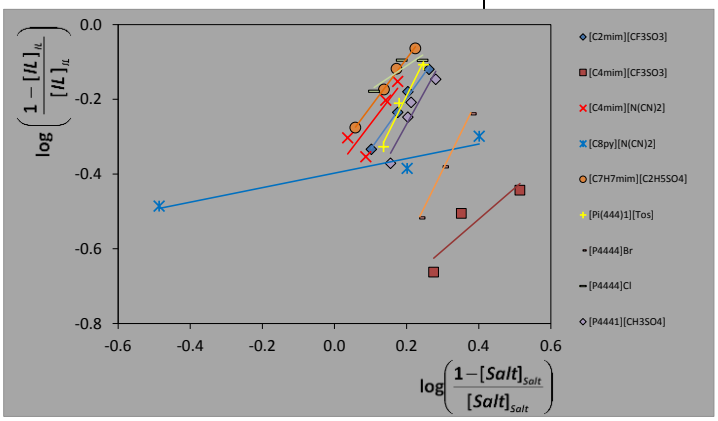

Figure S 4.2. Tie-lines correlation using the Othmer-Tobias correlation for each system composed of IL + $Al_2(SO_4)_3$ + H_2O.

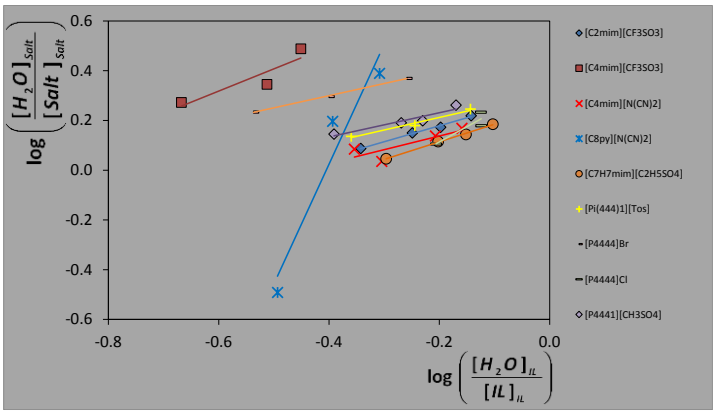

Figure S 4.3. Tie-lines correlation using the Bancroft correlation for each system composed of IL + $Al_2(SO_4)_3$ + H_2O.

References

1. J. D. Seader and E. J. Henley, Separation Process Principles, John Wiley & Sons, New York, 1998.

2. D. Othmer and P. Tobias, *Ind. Eng. Chem.*, 1942, **34**, 693–696.

3. J. P. O'Connell and J. M. Haile, Thermodynamics: Fundamentals for Applications, Cambridge University Press, New York, 2005.

4. J. M. Sørensen, T. Magnussen, P. Rasmussen, and A. Fredenslund, *Fluid Phase Equilib.*, 1979, **3**, 47–82.

5. A. Brooke, D. Ketndrick, A. Meeraus, and R. Raman, GAMS - A User's Guide, GAMS Development Corporation, Washington DC, 2005.

6. A. S. Drud, *ORSA J. Comput.*, 1992, **6**, 207–216.

7. 2010.

8. M. Tawarmalani and N. V Sahinidis, Convexification and Global Optimization in Continuous and Mixed-Integer Nonlinear Programming, Kluwer Academic Publishers, Dordrecht, 2002.

9. S. Seki, N. Serizawa, K. Hayamizu, S. Tsuzuki, Y. Umebayashi, K. Takei, and H. Miyashiro, *J. Electrochem. Soc.*, 2012, **159**, A967–A971.

10. Q.-S. Liu, J. Tong, Z.-C. Tan, U. Welz-Biermann, and J.-Z. Yang, *J. Chem. Eng. Data*, 2010, **55**, 2586–2589.

11. D. Almantariotis, S. Stevanovic, O. Fandiño, A. S. Pensado, A. A. H. Pádua, J.-Y. Coxam, and M. F. Costa Gomes, *J. Phys. Chem. B*, 2012, **116**, 7728–7738.

12. M. Součková, J. Klomfar, and J. Pátek, *J. Chem. Thermodyn.*, 2012, **48**, 267–275.

13. D. S. H. Wong, J. P. Chen, J. M. Chang, and C. H. Chou, *Fluid Phase Equilib.*, 2002, **194–197**, 1089–1095.

14. U. Domańska, M. Królikowski, A. Pobudkowska, and P. Bocheńska, *J. Chem. Thermodyn.*, 2012, **55**, 225–233.

15. G. A. Kaminski and W. L. Jorgensen, *J. Chem. Soc. Perkin Trans. 2*, 1999, 2365–2375.

16. J. N. Canongia Lopes, J. Deschamps, and A. A. H. Pádua, *J. Phys. Chem. B*, 2004, **108**, 2038–2047.

17. J. N. Canongia Lopes and A. A. H. Pádua, *J. Phys. Chem. B*, 2004, **108**, 16893–16898.

18. K. Shimizu, D. Almantariotis, M. F. Costa Gomes, A. A. H. Pádua, and J. N. Canongia Lopes, *J. Phys. Chem. B*, 2010, **114**, 3592–600.

19. P. González-Tello, F. Camacho, G. Blázquez, and F. J. Alarcón, *J. Chem. Eng. Data*, 1996, **41**, 1333–1336.